Nanoscale Advances

ROYAL SOCIETY OF CHEMISTRY

PAPER

View Article Online
View Journal | View Issue

Cite this: *Nanoscale Adv.*, 2026, **8**, 1851

Enhanced cytotoxic activity of *Moringa oleifera*-loaded pharmacosomes against neuroblastoma

Obaydah Abd Alkader Alabrahim, [a] Ahmed Maher Abdeldayem [ab] and Hassan Mohamed El-Said Azzazy *[ac]

Moringa oleifera is known for its diverse therapeutic properties, including anticancer effects attributed to its rich phytochemical profile; yet, its poor solubility and stability limit its therapeutic translation. In this study, phospholipid-based pharmacosomal nanocarriers loaded with *Moringa oleifera* extract (MO) were developed and characterized to enhance its delivery and anticancer efficacy against neuroblastoma. Neuroblastoma is a common pediatric malignancy of neural crest origin with poor prognosis in high-risk cases, highlighting the need for safer and more effective therapeutic strategies. GC-MS analysis of the MO extract revealed diverse bioactive constituents with documented cytotoxic, pro-apoptotic, and antioxidant properties, including polyphenolic acids, flavonoid derivatives, nootkatone, uridine, and fatty acid derivatives. MO-loaded pharmacosomes (MO-PhS) formulated using lecithin and chitosan exhibited favorable physicochemical characteristics, including nanoscale size (41.07–190.12 nm), high entrapment efficiency (94.52 ± 2.79%), spherical morphology (PDI 0.29 ± 0.04), strong negative surface charge (−58.73 ± 0.99 mV), and enhanced thermal stability. *In vitro* cytotoxicity studies on SH-SY5Y neuroblastoma cells demonstrated a marked enhancement in anticancer activity for MO-PhS, achieving approximately a 10-fold reduction in IC_{50} compared to free MO. Cell cycle analysis by flow cytometry revealed a pronounced redistribution of treated cells from G0/G1 into S and G2/M phases, indicating disruption of proliferative progression and replication stress, with pharmacosomal delivery of MO producing a more pronounced S-phase accumulation. Notably, these cell cycle perturbations were achieved at an approximately 10-fold lower concentration for MO-PhS compared to the free extract, underscoring the superior dose-efficiency of pharmacosomal delivery. Plain pharmacosomes exhibited minimal cytotoxicity against human normal fibroblasts (hFB), confirming carrier biocompatibility. These findings highlight MO-PhS as a promising nanoplatform for neuroblastoma therapy, offering enhanced cytotoxic efficacy, higher stability and antioxidant properties, and excellent biocompatibility, warranting further preclinical investigation.

Received 13th May 2025
Accepted 24th January 2026

DOI: 10.1039/d5na00473j

rsc.li/nanoscale-advances

1. Introduction

Neuroblastoma is the most common extracranial solid tumor occurring in childhood and accounts for 15% of pediatric cancer deaths.[1,2] Despite advances in chemotherapy, radiotherapy, and surgical interventions, high-risk neuroblastoma remains associated with poor long-term survival and significant treatment-related toxicity.[2] Thus, there is a critical need for novel, safe, and more effective therapeutic strategies that target tumor cells while minimizing systemic side effects.

Natural products derived from medicinal plants have gained increasing attention for cancer treatment, offering diverse bioactive compounds with antioxidant, anti-inflammatory, and cytotoxic activities.[3,4] Commonly recognized as the "tree of life" or "miracle tree", *Moringa oleifera* is widely utilized as a functional food and nutritional supplement around the world.[5–8] *M. oleifera* has been extensively used in traditional and ethnomedicine, which suggests that it may have multifaceted preventive and therapeutic activities against a wide range of human disorders.[5–8] In fact, *M. oleifera*, particularly leaves, has been positively correlated with a number of pharmacological benefits, showing outstanding therapeutic activities such as antihypertensive, antispasmodic, anticoagulant, antiviral, antidiabetic, antiulcer, antipyretic, anti-inflammatory, antimicrobial, anticancer, hepatoprotective, immunostimulant, and cardiotonic effects.[5–15]

Moreover, *M. oleifera* compromises plenty of vitamins, oils, proteins, minerals, lipids, metal ions, and phenolic ingredients. Phenolic compounds entailed are mostly carotenoids, flavonoids, and phenolic acids, which are effective against

[a]*Department of Chemistry, School of Sciences & Engineering, The American University in Cairo, AUC Avenue, SSE # 1184, P.O. Box 74, New Cairo 11835, Egypt. E-mail: hazzazy@aucegypt.edu; Tel: +20 02 2615 2559*

[b]*Biotechnology Department, Faculty of Science, Cairo University, Giza, Egypt*

[c]*Department of Nanobiophotonics, Leibniz Institute of Photonic Technology, Jena, Germany*

malnutrition and other illnesses.[16–23] Significantly, the United Nations has recommended using *M. oleifera* as a nutritional supplement to the human diet, supporting the high safety profile of this plant.[24] Also, a daily intake of 1 g Kg^{-1} of *M. oleifera* has been reported to be safe for human consumption.[25] Recent experimental investigations reported neuroprotective effects of *M. oleifera* against several neurodegenerative disorders, including dementia,[26] Alzheimer's disease,[27,28] PD,[29–31] and stroke.[32,33]

Furthermore, *M. oleifera* has been shown to contain several phytochemicals such as flavonoids, phenolics, sterols, fatty acids, and terpenoids, many of which have shown cytotoxicity against various cancer cell lines, including breast, colon, and liver cancers.[34–36] Also, the cytotoxic effects of *M. oleifera* have been explained by several mechanisms exerted by its extracts, including significant suppression in Nrf2 mRNA level and a corresponding decrease in protein expression, intracellular induction of ROS and reduction of glutathione levels, and promotion of pro-apoptotic action (*via* increase in p53 protein expression, caspase-9, caspase-3/7 activities, *etc.*) in tumor cells.[34–36] These mechanisms strongly support the role of *M. oleifera* in antiproliferation and potent induction of apoptosis in cancer cells.

Nevertheless, the main challenges facing the clinical applications of natural extracts, including *M. oleifera*, generally include poor aqueous solubility, low bioavailability, and limited stability in physiological environments.[12,19,37,38] To overcome these limitations, the use of nanocarrier systems has emerged as a promising approach to enhance the delivery and efficacy of plant-derived compounds.

Pharmacosomes, a class of lipid-based nanocarriers composed of phospholipid complexes (typically lecithin) and stabilizing agents such as chitosan, offer several advantages for drug delivery, including enhanced solubility, stability, site-specific targeting, and controlled release.[39–42] They share similar structural characteristics with lipid-based nanocarriers, particularly the presence of a bilayer membrane, allowing them to effectively encapsulate both hydrophilic and lipophilic agents. This dual loading capacity enhances the solubility, stability, and bioavailability of poorly water-soluble natural extracts, while also improving controlled release and site-specific targeting.[39,40]

In comparison to conventional liposomes, pharmacosomes offer several advantages, including superior physicochemical stability, less susceptibility to oxidative degradation, and improved drug entrapment efficiency.[39,40,43] Moreover, their reduced likelihood of drug leakage during storage or circulation contributes to better shelf life and therapeutic performance, features particularly important for natural products such as *M. oleifera* extracts, which often exhibit poor pharmacokinetic profiles and instability under physiological conditions.[44] Additionally, pharmacosomes do not require cholesterol for bilayer stabilization, which minimizes formulation complexity and potential interference with bioactivity. Their self-assembling ability and relatively simple preparation methods further support their scalability and industrial feasibility.[39,40]

In addition to improved stability and delivery efficiency, pharmacosomes are reported to enhance the cytotoxic efficacy of loaded bioactives by promoting stronger membrane interaction, improved intracellular accumulation, and sustained exposure of tumor cells to therapeutic compounds. Such features have translated into greater antiproliferative and pro-apoptotic activity compared to free drugs or conventional lipid carriers in several cancer models.[39] Also, pharmacosomes exhibit enhanced targeting efficiency, making them particularly suitable for treating and targeting various malignancies including neuroblastoma. Their nanoscale size and optimized surface characteristics can facilitate enhanced permeability and retention (EPR) in tumor tissues and potentially support targeted delivery for treating cancers such as neuroblastoma.[45] Recent studies have demonstrated that pharmacosome formulations significantly increase BBB penetration and brain accumulation of therapeutic agents, supporting their application in neurological disorders.[45]

In this study, pharmacosome nanoparticles were prepared as a delivery system for *M. oleifera* extract. Their physicochemical properties, thermal stability, antioxidant capacity, and cytotoxic activity against SH-SY5Y neuroblastoma cells were investigated, aiming to explore their potential as a natural-product-based anticancer platform for treating neuroblastoma.

2. Materials and cell culture

2.1. Materials

Fresh leaves of *M. oleifera* were purchased from a local vendor (Cairo, Egypt). Lecithin was purchased from VWR BDH Chemicals (Fontenay-sous-Bois, France). Low molecular weight chitosan was supplied by CDH Fine Chemicals (New Delhi, India). Phosphate buffer saline (PBS) tablets were supplied by Genetix (Genetix Biotech, Asia, Pvt., Ltd). Chloroform was purchased from Chem-Lab NV, Belgium. DPPH was provided by Sigma (Sigma-Aldrich Co., Germany). DMSO was obtained from Fisher Scientific (UK). KBr (FTIR grade) was purchased from Merck (KGaA, Darmstadt, Germany). MTT was provided by SERVA GmbH (USA). Dimethyl sulfoxide (DMSO) was obtained from Merck (Darmstadt, Germany).

2.2. Cell culture

SH-SY5Y cells, isolated from a bone marrow biopsy taken from a four-year-old female with neuroblastoma, were purchased from ATCC, USA. The cells were routinely cultured in high-glucose DMEM. It was supplemented with 10% fetal bovine serum (FBS), 2 mM L-glutamine, and contained 100 units per mL of penicillin G sodium and 100 units per mL of streptomycin sulphate. All from PAN-Biotech, (Germany). Cells were maintained at sub-confluency at 37 °C in humidified air containing 5% CO_2. For sub-culturing, monolayer cells were harvested after trypsin/EDTA treatment at 37 °C. Cells were used when confluence had reached 75%.[46]

3. Methods

3.1. Preparation and Soxhlet extraction of *Moringa oleifera* leaf extract (MO)

Fresh *M. oleifera* leaves were thoroughly washed with tap water to remove surface impurities and subsequently air-dried in

a dark, well-ventilated environment at 20 °C to preserve their bioactive compounds. Once dried, the leaves were finely ground into a uniform powder using a high-speed blender and stored under refrigeration for further use. For extraction, the Soxhlet method was employed, utilizing a 90% (v/v) methanolic solution as the solvent. A leaf powder-to-solvent ratio of 1 g per 10 mL of methanol (90%) was maintained, and the extraction process was carried out at a controlled temperature range of 60–70 °C. The extraction continued for approximately 9 h until the solvent exhibited a pale greenish coloration, indicating the depletion of soluble compounds. The obtained *M. oleifera* extract (MO) was subsequently collected, dried in a desiccator at ambient temperature, and stored at 4 °C to retain its stability and bioactivity.[47]

3.2. Preparation of pharmacosome nanostructures

Three pharmacosome formulations (PhS1, PhS2, and PhS3) were prepared using the thin-film hydration method, with some modifications.[45] In each formulation, lecithin and low molecular weight chitosan were dissolved in 5 mL of tetrahydrofuran (THF) inside a sealed glass container. The mixture was then transferred into a 100 mL round-bottom flask and subjected to rotary evaporation (45 min) until a thin lipid film was formed on the flask walls. The lipid film was then hydrated using phosphate-buffered saline (PBS, pH 7.4) under rotary evaporation for at least 1 h to ensure complete hydration. The final pharmacosome dispersions were stored at 4 °C for further characterization. PhS1 and PhS2 varied in lecithin concentration, whereas PhS3 incorporated 0.4% (w/v) of MO extract into the formulation (Table 1).

3.3. Characterization tests

3.3.1. GC-MS analysis. The MO extract was derivatized with bis(trimethylsilyl)trifluoroacetamide (300 μL, 80 °C, 2 h) to volatilize polar compounds. Chromatographic separation was performed on an Agilent 7890B GC/5977A MSD system equipped with an HP-5MS capillary column (30 m × 0.25 mm × 0.25 μm). Helium carrier gas was maintained at 8.2 psi (constant pressure mode). The oven program was held at 60 °C for 5 min, ramped at 20 °C min^{-1} to 300 °C, and held for 5 min. Injection was performed in split-less mode (1 μL, 300 °C). Mass spectrometry operated in electron ionization (EI) mode (70 eV), scanning *m*/*z* 50–550 with an 8.0 min solvent delay (ion source: 230 °C; quadrupole: 150 °C). Compounds were identified using the NIST/EPA/NIH mass spectral library (v2.2, 2014) with ≥80% similarity matching.[48,49]

3.3.2. Fourier transform infrared (FTIR) spectroscopic characterization. FTIR spectroscopy was employed to chemically characterize the MO extract, plain pharmacosomes (PhS), and MO-loaded pharmacosomes (MO-PhS). Analysis was conducted using a Nicolet 380 FTIR (Thermo-Scientific, Madison, USA), applying the potassium bromide (KBr) disc method. Spectral data were recorded within the frequency range of 4000–400 cm^{-1} at a resolution of 4 cm^{-1}.

3.3.3. Thermogravimetric analysis (TGA). The thermal stability and degradation behavior of the MO extract and both plain and loaded pharmacosomal nanoformulations were assessed using a TGA Q50 thermogravimetric analyzer (TA Instruments, New Castle, DE, USA). Accurately weighed samples were subjected to a controlled heating process from 25 °C to 600 °C at a constant rate of 10 °C min^{-1} under a nitrogen atmosphere (flow rate: 50 mL min^{-1}). The corresponding weight loss of each sample was continuously recorded as a function of temperature, providing insights into their thermal decomposition profiles.

3.3.4. Nanoparticle morphology and encapsulation analysis by UHR-TEM. The encapsulation efficiency of MO extract within MO-PhS and their morphological characteristics were examined using ultra-high resolution transmission electron microscopy (UHR-TEM) (JEOL JEM-2100 Plus, Tokyo, Japan) operated at 200 kV, following established protocols for lipid-based nanoparticles. Briefly, nanoparticle suspensions were prepared in distilled water, sonicated (37 °C, 10 min), and deposited onto 200-mesh copper grids coated with a 1 nm carbon film. Samples were negatively stained with 2% (w/v) uranyl acetate for 30 s, blotted dry with filter paper, and air-dried prior to imaging. Morphological analysis was performed at magnifications ranging from 5000× to 1 000 00× to assess nanoparticle size, uniformity, and encapsulation integrity.

3.3.5. Dynamic light scattering (DLS) and zeta potential analysis. The hydrodynamic diameter (Z-average), polydispersity index (PDI), and zeta potential of both PhS and MO-PhS were characterized using a Nano-Zetasizer system (Malvern Instruments Ltd, UK). For DLS measurements, samples were diluted in phosphate-buffered saline (PBS) (1 : 10, w/v) and analyzed at 25 °C. Zeta potential was measured in the same instrument using laser Doppler electrophoresis, with samples appropriately dispersed in PBS to maintain consistent ionic strength. All measurements were performed in triplicate.

3.3.6. Encapsulation efficiency (EE%) determination. The encapsulation efficiency (EE%) of MO extract in pharmacosomes was determined using an indirect ultraviolet

Table 1 Composition of pharmacosome formulations. (The concentration of *Moringa* extract in PhS3 was selected based on initial screening studies conducted on neuroblastoma cells)[a]

Formulation	Lecithin (% w/v)	Chitosan (% w/v)	MO (% w/v)	Solvent (THF)	Hydration medium (PBS, pH 7.4)
PhS1	4.5%	0.25%	—	5 mL	5 mL
PhS2	2.25%	0.25%	—	5 mL	5 mL
PhS3	2.25%	0.25%	0.4%	5 mL	5 mL

[a] Abbreviations: THF = tetrahydrofuran; PBS = phosphate buffer saline; PhS = pharmacosomes; MO = *Moringa oleifera* leaf extract.

spectrophotometric method. Briefly, nanoparticle suspensions (MO-PhS) were centrifuged at 15 000 rpm for 1.5 hours at 4 °C to separate unencapsulated phytochemicals. The absorbance of the collected supernatant was measured at 330 nm using a FLUOstar Omega microplate reader (BMG Labtech, Germany). This wavelength was selected to target a range of cytotoxic constituents, including phenolic acids and flavonoids, identified in the extract *via* GC-MS analysis, such as ferulic acid and chlorogenic acid. A calibration curve was constructed ($y = 0.0017x + 0.1421$, $R^2 = 0.9905$) to quantify the concentration of free phenolic acids and flavonoids, enabling indirect calculation of encapsulation efficiency. Encapsulation efficiency was calculated using the following equation:

$$\text{EE\%} = \frac{\text{Total MO} - \text{Free MO}}{\text{Total MO}} \times 100$$

where Total MO represents the initial concentration of *Moringa oleifera* extract, and Free MO corresponds to the unencapsulated fraction, as determined from the supernatant absorbance measurements.

3.4. Biological assessment assays

3.4.1. Antioxidant activity assessment. The antioxidant potential of the MO extract was evaluated using the 1,1-diphenyl-2-picrylhydrazyl (DPPH) assay. Serial dilutions of the extract were prepared at concentrations ranging from 15.625 μg mL^{-1} to 1 mg mL^{-1} and mixed with an equal volume (1 : 1, v/v) of a 0.12 mM methanolic DPPH solution. The reaction mixtures were then incubated in darkness at room temperature for 30 minutes. Following incubation, the absorbance was measured spectrophotometrically at 517 nm (Cary 3500 UV-Vis Engine, Agilent Technologies, Pty Ltd, Mulgrave, Australia). The DPPH radical scavenging activity was calculated using the equation below, where A_β represents the absorbance of the DPPH methanolic solution (blank) and A_s denotes the absorbance of the sample mixture:

$$\%\text{DPPH scavenging activity} = \frac{A_\beta - A_s}{A_\beta} \times 100$$

3.4.2. Biocompatibility assay against hFB cells. Normal human fibroblast (hFB) cell line was purchased from Rio de Janeiro Cell Bank (BCRJ, Brazil). Cells were cultured in high-glucose Dulbecco's Modified Eagle Medium (DMEM), which comprised 10% fetal bovine serum (FBS), 2 mM L-glutamine, and 1% antibiotic-antimycotic cocktail. All were purchased from PAN-Biotech (Germany). Cells were maintained at sub-confluency in humidified air containing 5% CO_2 at 37 °C. For the subculturing step, monolayer cells were treated with trypsin/EDTA and harvested at 37 °C. Cells were used upon reaching 75% confluency.[50]

3.4.3. Cytotoxicity assay. The cytotoxicity of the tested samples was evaluated using the MTT assay (3-[4,5-dimethylthiazole-2-yl]-2,5-diphenyltetrazolium bromide). This colorimetric method relies on the ability of mitochondrial dehydrogenase enzymes in viable cells to reduce the yellow MTT dye into insoluble dark blue formazan crystals. The amount of formazan formed after solubilization correlates directly with the number of metabolically active (viable) cells. Briefly, cells (1×10^4 cells per well) were seeded into flat-bottom 96-well microplates and incubated overnight to allow attachment. Subsequently, cells were treated with 50 μL of varying concentrations of the tested samples, including MO extract, plain PhS, and MO-PhS nanoparticles, at final concentrations of 15.625, 31.25, 62.5, 125, 250, 500, and 1000 μg mL^{-1}. Treatments were performed in triplicate and incubated for 48 h at 37 °C in a humidified 5% CO_2 atmosphere. After incubation, the media were removed, and 50 μL of MTT solution (5 mg mL^{-1}) was added to each well and incubated for an additional 4 h under the same conditions. The resulting formazan crystals were solubilized by adding 150 μL of dimethyl sulfoxide (DMSO) per well. Plates were shaken gently at room temperature to ensure complete dissolution, followed by measurement of absorbance at 560 nm using a microplate ELISA reader (FLUOstar OPTIMA, BMG LABTECH GmbH, Ortenberg, Germany). All experiments were performed in triplicate, and average values were calculated.[51] The percentage of relative cell viability was determined using the following equation:

$$\text{Cell viability\%} = \frac{\text{Absorbance of treated cells}}{\text{Absorbance of control cells}} \times 100$$

The half-maximal inhibitory concentration (IC_{50}) was then calculated from the equation of the dose–response curve.

3.4.4. Flow cytometry analysis of cell cycle distribution. SH-SY5Y human neuroblastoma cells were seeded in 6-well plates and allowed to adhere for 24 h. Cells were then treated with MO extract and MO-PhS nanoparticles at their respective IC_{50} concentrations, as previously determined by the MTT assay. Untreated cells served as the negative control. After 48 h of treatment, cells were harvested, washed with DPBS (Dulbecco's phosphate-buffered saline), trypsinized (0.05% trypsin–EDTA), and fixed in ethanol. Cell cycle analysis was performed using a Beckman Coulter Cell Cycle Analysis Kit (Cat. No. PN 4238055-CB), followed by propidium iodide staining. DNA content was analyzed using a CytoFLEX flow cytometer (Beckman Coulter Life Sciences, USA), and cell populations were quantified in G0/G1, S, and G2/M phases using the associated analysis software.[50]

3.5. Statistical studies

The results were reported as mean ± standard deviation (SD). All formulations were prepared in triplicate. ImageJ software was used to analyze the particle size distribution of the obtained nanoparticles. Dose–response curves were generated using non-linear regression analysis with an asymmetric five-parameter logistic model: X = log(concentration), employing GraphPad Prism version 10.3.0 (507) for Windows (GraphPad Software, San Diego, CA, USA).

4. Results and discussion

4.1. GC-MS results and anticancer relevance of identified compounds against various tumors

The GC-MS analysis of the MO extract revealed a diverse array of phytochemicals (Fig. 1, S1 and Table 2), comprising several

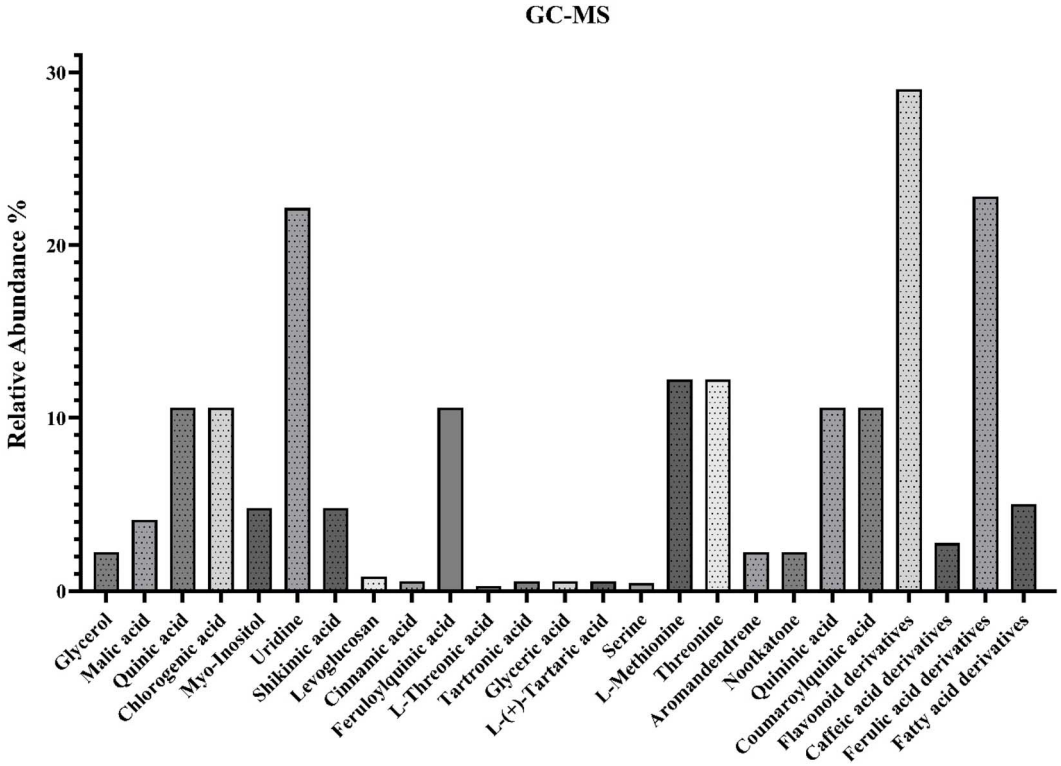

Fig. 1 Key identified compounds in the MO extract.

compounds with previously reported anticancer properties relevant to different malignancies. These results offer a compelling biochemical rationale for utilizing the extract in nanosystems aimed at treating neuroblastoma.

Among the predominant compounds, uridine (22.16%) has demonstrated anti-tumor activity through its role in nucleotide metabolism, modulation of DNA/RNA repair mechanisms, enhancement of chemotherapeutic efficacy, and induction of ferroptosis. It is also involved in regulating tumor cell proliferation and survival, particularly in glioma and neuroblastoma models.[52–56]

The extract also contained significant levels of phenolic acids, including feruloylquinic acid, chlorogenic acid, and quinic acid (10.6%). These compounds are recognized for their antioxidant properties and pro-apoptotic effects in cancer cells. Markedly, chlorogenic acid has been shown to induce apoptosis and cell-cycle arrest at the G2/M phase in glioma U373 cells, as well as suppress migration and invasion by modulating the SRC/MAPKs signaling pathway.[57]

Myo-inositol (4.81%) and shikimic acid (4.82%) were also notable, both recognized for their cytotoxic effects and potential anticancer roles.[58–61] For instance, myo-inositol has demonstrated broad-spectrum anticancer potential by modulating critical pathways such as PI3K/Akt, disrupting growth factor signaling, and interfering with cytoskeletal dynamics. These effects collectively inhibit tumor progression and metastasis.[58]

The extract also contained substantial amounts of flavonoid derivatives (29.02%) and ferulic acid derivatives (22.83%), which are well-documented for their cytotoxic effects, DNA damage induction, and selective apoptosis of tumor cells, including neuroblastoma and glioblastoma. These compounds are known to downregulate pro-survival genes and enhance ROS-mediated cytotoxicity in cancer cells.[62–70]

Additionally, nootkatone (2.25%) was also detected. It is a promising sesquiterpene that exhibited antiproliferative activity in colorectal cancer cells.[71,72] Other minor but relevant compounds included caffeic acid derivatives, coumaroylquinic acid, and fatty acid derivatives such as oleic acid. Oleic acid has been shown to inhibit fatty acid and cholesterol synthesis in glioma cells, potentially contributing to the suppression of tumor growth.[73]

Overall, the chemical profile revealed by GC-MS supports the anticancer potential of the MO extract and its integration into nanocarrier systems targeting several tumors, including neuroblastoma.

4.2. Morphological and physicochemical characterization of the nanoparticles

Ultra-high-resolution transmission electron microscopy (UHR-TEM) was employed to assess the morphological characteristics and confirm the nanoscale size of the developed formulations, alongside verifying the successful encapsulation of the MO extract. As illustrated in Fig. 2, TEM images for both plain pharmacosomes (PhS2) and MO-loaded pharmacosomes (PhS3) revealed well-dispersed, spherical nanostructures with smooth contours. The particle sizes observed were noticeably smaller, ranging from 41.07–190.12 nm for PhS2 and 26.05–211.08 nm for PhS3, and more uniform than those recorded by dynamic

Table 2 List of bioactive compounds identified in the MO extract *via* GC-MS, with corresponding retention times (RT), peak numbers, and relative abundance[abc]

No.	Compound name	MW (g mol^{-1})	CAS number	RT (min)	Peak	Relative abundance (%)	Biological activity
1	Glycerol	92.09	56-81-5	9.632	1	2.25%	Precursor for lipid synthesis; may influence tumor cell membrane dynamics
2	Malic acid	134.09	6915-15-7	11.189	3	4.13%	Showed anticarcinogenic effect on glioblastoma cells *via* the necrotic pathway and apoptotic properties on fibroblast cells
3	Quinic acid	192.17	77-95-2	13.249	13	10.6%	Has antioxidant activity that has shown anticancer properties through apoptosis-mediated cytotoxicity in breast cancer cells. Also, derivatives of quinic acid exhibited cytotoxic effects against glioblastoma cells by inducing apoptosis
4	Chlorogenic acid	354.31	327-97-9	13.249	13	10.6%	Induced differentiation and apoptosis in glioma cells; inhibited tumor growth *in vivo*
5	Myo-inositol	180.16	87-89-8	15.434	15	4.81%	Exhibited broad-spectrum anticancer activity; modulated PI3K/Akt pathway and inhibited tumor invasiveness
6	Uridine	244.20	58-96-8	16.401	32	22.16%	Inhibited hepatocellular carcinoma cell development by inducing ferroptosis
7	Shikimic acid	174.15	138-59-0	14.805	22	4.82%	Exhibited anticancer effects *via* suppressing migration and invasion, inducing apoptosis, and inhibiting proliferation in colorectal cancer cells. Additionally, derivatives of shikimic acid exhibited cytotoxic effects against liver cancer cells
8	Levoglucosan	162.14	498-07-7	12.533	8	0.84%	Derivatives showed cytotoxic activities against several sorts of cancers (lung, colon, and hepatocarcinoma cells)
9	Cinnamic acid	148.16	140-10-3	10.084	2	0.58%	Antioxidant phenolic acid. Induced cytostasis and differentiation in glioblastoma cells and other cancerous cells (melanoma, prostate and lung); inhibited tumor invasiveness
10	Feruloylquinic acid	368.3	62 929-69-5	13.249	13	10.6%	Limited direct evidence on anticancer activity; feruloylquinic acid and its derivatives exhibited antioxidant properties; showed neuroprotective effects
11	L-threonic acid	136.11	3909-12-4	11.48	4	0.29%	Limited direct evidence on anticancer activity; known for its antioxidant properties (vitamin C synergist)
12	Tartronic acid	120.06	80-69-3	10.084	2	0.58%	Limited direct evidence on anticancer activity; may inhibit lipid peroxidation
13	Glyceric acid	106.08	473-81-4	10.084	2	0.58%	Limited direct evidence on anticancer activity; involved in metabolic pathways. Glutathione precursor
14	L-(+)-Tartaric acid	150.09	87-69-4	10.084	2	0.58%	Limited direct evidence on anticancer activity; functions as a metal chelator
15	Serine	105.09	56-45-1	11.795	6	0.47%	Essential amino acid. Glutathione precursor
16	L-Methionine	149.21	63-68-3	12.814	10	12.23%	Sulfur-containing amino acid with antioxidant roles
17	Threonine	119.12	72-19-5	12.814	10	12.23%	Essential amino acid contributes to membrane integrity
18	Aromandendrene	204.35	489-39-4	9.632	1	2.25%	Anti-inflammatory terpene, with various anticancer properties

Table 2 (*Contd.*)

No.	Compound name	MW (g mol^{-1})	CAS number	RT (min)	Peak	Relative abundance (%)	Biological activity
19	Nootkatone	218.34	4674-50-4	9.632	1	2.25%	A sesquiterpene compound. Exhibited antiproliferative activity in colorectal cancer cells. Showed promising neuroprotective effects while improving cognitive function in Alzheimer's disease models
20	Coumaroylquinic acid	338.31	32 451-86-8	13.249	13	10.6%	Polyphenolic ester; mitochondrial protective effects
21	Flavonoid derivatives	∼500–600	N/A	12.5–15	7, 18	29.02%	General class includes compounds with broad-spectrum anticancer activity; induce apoptosis in brain tumor cells
22	Caffeic acid derivatives	∼350–400	N/A	10–14	5, 9	2.78%	Antioxidant polyphenols with hydroxyl groups. Induced apoptosis in cancer cells; inhibit tumor growth
23	Ferulic acid derivatives	∼400–450	N/A	12–14	10, 13	22.83%	Neuroprotective and anti-inflammatory polyphenols. Inhibited angiogenesis and tumor growth; induced apoptosis in cancer cells
24	Fatty acid derivatives (oleic acid)	354.6	21 556-26-3	15.24	23	5.02%	Contribute to cell membrane stability and function. Also, oleic acid showed anticancer activity against different carcinomas

[a] Retention times represent TMS-derivatized forms as identified by GC-MS analysis. [b] Some peaks correspond to multiple co-eluted compounds or broad compound classes (*e.g.*, flavonoid, caffeic acid, and ferulic acid derivatives), as detected by spectral matching in the GC-MS analysis. Peak numbers reflect those assigned in the original chromatogram. [c] Molecular weights (MWs) and CAS numbers refer to the native, non-derivatized forms of the compounds. All MWs and CAS numbers were verified against authoritative chemical databases (PubChem, ChemSpider, Sigma-Aldrich). Approximate MWs (∼) are given where specific compound structures could not be assigned.

light scattering (DLS), suggesting the rare presence of aggregations and supporting successful formulation.

More importantly, MO-loaded pharmacosomes (PhS3) displayed a compact morphology with a more condensed structure, potentially indicating encapsulation and interaction between the MO extract and the lipid/chitosan matrix of the pharmacosomes. These visual cues also imply enhanced structural integrity, which is critical for biological applications, particularly in terms of cellular uptake and systemic circulation stability.[74,75]

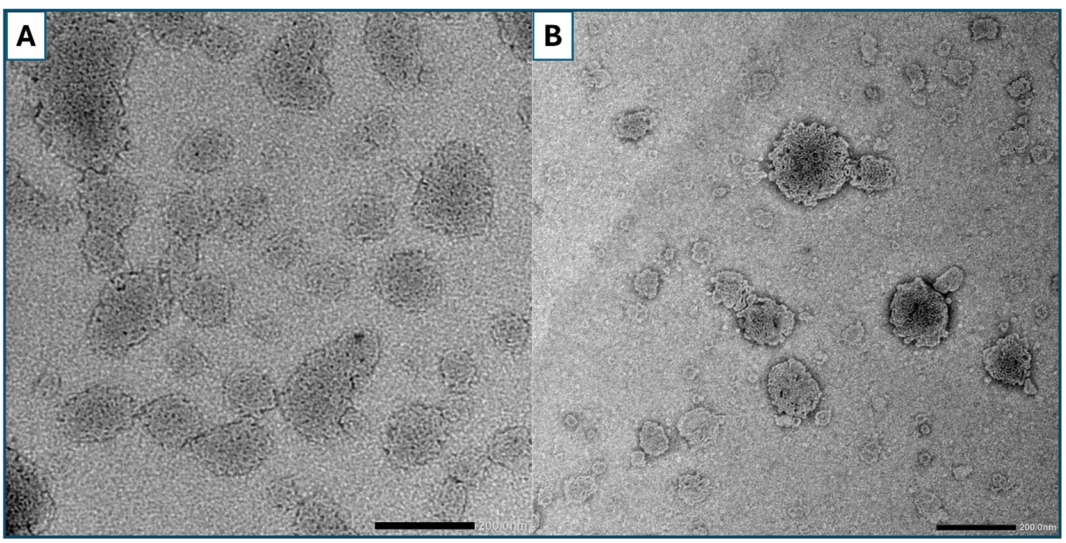

Fig. 2 Ultra-high-resolution transmission electron microscopy (UHR-TEM) images of (A) plain pharmacosome nanoparticles (PhS2) and (B) MO-loaded pharmacosome nanoparticles (PhS3). All images are shown with a 200 nm scale bar. Panel A displays unloaded nanoparticles with well-defined spherical to slightly oval morphology and minimal aggregation. Panel B illustrates MO-loaded pharmacosomes exhibiting enhanced structural compactness and denser appearance, indicative of successful MO extract encapsulation and integration within the lipid/chitosan matrix.

In contrast, DLS analysis yielded comparatively larger hydrodynamic diameters for all formulations, a discrepancy commonly attributed to the solvation layer and Brownian motion during measurement.[76,77] PhS1, with the highest lecithin content (4.5%), showed the largest Z-average values (255.67 ± 3.16 nm), the lowest surface charge (−29.93 ± 0.47 mV), and a comparable polydisperse profile (PDI 0.47 ± 0.019), suggesting that lecithin enrichment contributes to vesicle enlargement and reduced electrostatic repulsion. PhS2 and PhS3, with equal lecithin content but differing in MO presence in PhS3, demonstrated distinct size and charge profiles. PhS2 showed a more compact profile (average size of 190.4 ± 0.78 nm, PDI of 0.29 ± 0.04, and zeta potential of −58.73 ± 0.99 mV), while PhS3 presented a broader size distribution (280.93 ± 3.11 nm *Z*-average, 0.68 ± 0.08 PDI, and −55.73 ± 0.06 mV zeta potential). The high surface charge of PhS2 and PhS3 reflects strong electrostatic stabilization, likely imparted by both the phosphate groups of lecithin and the protonated amines of low molecular weight chitosan.[78,79]

Interestingly, despite PhS3 (MO-loaded pharmacosomes) showing a broader size distribution by DLS, its corresponding TEM images revealed a more uniform and densely packed particle population. This disparity highlights the influence of formulation conditions (*e.g.*, sonication, dilution, and dispersing medium) on hydrodynamic measurements, while emphasizing that TEM provides a more accurate representation of dry-state morphology.[80]

From a functional standpoint, these nanoparticulate properties directly influence therapeutic performance. The reduced particle size and stable surface charge observed in MO-loaded pharmacosomes suggest efficient cellular internalization *via* endocytosis, particularly in neuroblastoma cells (SH-SY5Y), which possess high membrane fluidity and active endocytic pathways. Additionally, the negative surface potential aids in prolonged circulation by reducing opsonization and reticuloendothelial clearance.[81] Notably, the observed nanometric size range (<300 nm), as confirmed by TEM, combined with the high zeta potential, indicates a strong potential for targeting tumor cells, including neuroblastoma. Encapsulation within the lipid matrix may further support receptor-mediated uptake and membrane fusion processes in neural cells, thereby enhancing selective cytotoxic delivery to tumor tissue.[82,83]

4.3. Encapsulation efficiency of MO-loaded pharmacosomes (MO-PhS)

Encapsulation efficiency (EE%) of MO-PhS was quantified using an indirect UV-spectrophotometric method, as described in the methodology. The optimized formulation demonstrated a notably high EE% of 94.52 ± 2.79%, confirming the efficient entrapment of the constituents of MO extract within the pharmacosomal system.

This high EE% suggests a strong affinity between the *Moringa* phytochemicals and the lipid–chitosan matrix, likely facilitated by both hydrophilic and lipophilic interactions. The amphiphilic nature of the carrier system further contributed to this enhanced encapsulation, stabilizing a wide spectrum of phenolic compounds and flavonoids previously identified in the extract. This observation is supported by previous findings; Huang *et al.* (2017) demonstrated that liposomal encapsulation significantly improves the stability and retention of flavonoids such as quercetin and luteolin. Their study highlighted that interactions between flavonoids and the lipid bilayer enhance encapsulation efficiency and protect the compounds from degradation.[84]

From a therapeutic perspective, this high encapsulation performance is crucial for maximizing bioavailability and ensuring efficient delivery to neuroblastoma cells. SH-SY5Y cells, characterized by their active endocytic behavior and high membrane fluidity, are likely to internalize these pharmacosomal nanoparticles effectively, enabling enhanced intracellular accumulation of cytotoxic phytoconstituents. Encapsulation also plays a protective role, shielding sensitive compounds from premature degradation and metabolic inactivation, an essential aspect in tumor targeting, where stability and sustained intracellular presence are required for cytotoxic efficacy. Sengupta *et al.* (2021) reviewed the benefits of liposomal encapsulation of phenolic compounds, emphasizing improved bioavailability, enhanced neuronal uptake, and protection from premature degradation.[85]

4.4. FTIR spectroscopic characterization

The FTIR spectrum of the MO extract reveals several characteristic absorption bands indicative of its rich phytochemical composition. A broad O–H stretching vibration appears around 3300–3400 cm^{-1}, signifying the presence of hydroxyl groups from phenolic compounds and alcohols. Additionally, C–H stretching vibrations are observed near 2900 cm^{-1}, corresponding to aliphatic chains. The spectrum also displays a prominent C=O stretching band around 1700–1650 cm^{-1}, which can be attributed to carbonyl groups in flavonoids, aldehydes, or carboxylic acids. Aromatic C=C stretching vibrations emerge in the 1600–1500 cm^{-1} region, while C–O–C and C–OH stretching bands appear between 1100 and 1000 cm^{-1}, indicating the presence of ethers and alcohols. These findings align with previous studies that have identified similar functional groups in *Moringa* leaf extracts.[86,87]

The FTIR spectrum of the plain pharmacosomes (PhS) exhibits distinct bands characteristic of phospholipid structures. A broad band near 3300 cm^{-1} suggests N–H or O–H stretching, possibly from amine or hydroxyl groups in the phospholipids. Strong C–H stretching vibrations are evident around 2920–2850 cm^{-1}, corresponding to the lipid alkyl chains. A significant peak at approximately 1735 cm^{-1} indicates ester C=O stretching, a hallmark of phospholipid ester bonds. Notably, phosphoryl stretching (P=O) vibrations are observed near 1240 cm^{-1}, and phosphoester bond stretching (P–O–C) appears around 1092 cm^{-1}, confirming the presence of phosphate groups integral to the phospholipid structure.[88]

The FTIR spectrum of the MO-loaded pharmacosomes (MO-PhS) combines features from both the *Moringa* extract and plain pharmacosomes spectra, indicating encapsulation of the extract within the nanoparticles. The broad O–H stretching band

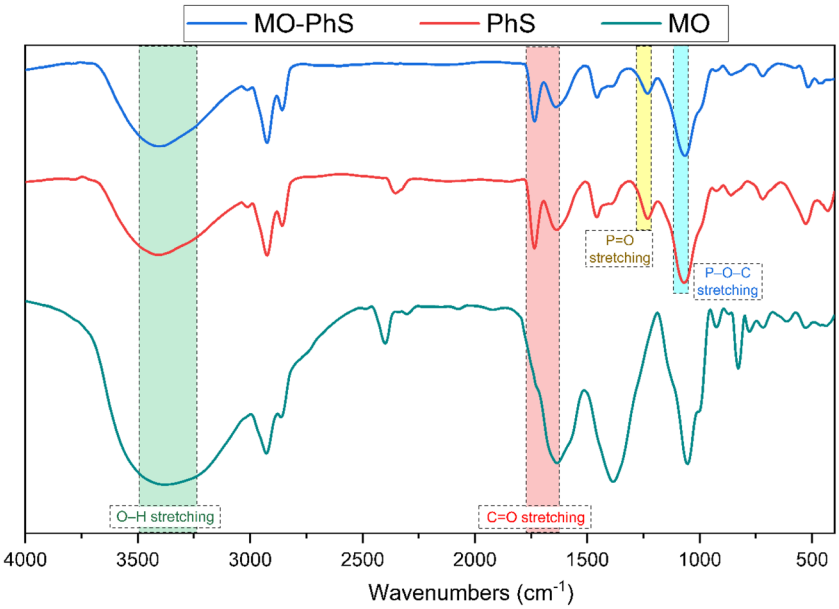

Fig. 3 FTIR spectra of *Moringa* extract (MO), plain pharmacosomes (PhS), and MO-loaded pharmacosomes (MO-PhS), highlighting key spectral bands. The shaded green region (3200–3500 cm^{-1}) corresponds to O–H stretching, showing broadening in MO-PhS indicative of hydrogen bonding between hydroxyl-rich phytoconstituents and lipid components. The red region (~1700 cm^{-1}) marks the C=O stretching band, with notable shifts and intensity changes post-encapsulation due to overlapping signals from phenolic and ester carbonyls. The yellow (~1240 cm^{-1}) and blue (~1090 cm^{-1}) regions represent P=O and P–O–C stretching vibrations, respectively, which are retained in both PhS and MO-PhS, supporting the preservation of the phospholipid bilayer's integrity and suggesting potential electrostatic or hydrogen-bond interactions with the extract. These findings collectively confirm the successful incorporation of MO constituents into the pharmacosomal matrix.

around 3300 cm^{-1} is retained but exhibits slight shifts and broadening, suggesting hydrogen bonding interactions between *Moringa* phenolics and phospholipid molecules. The ester C=O stretching band near 1730 cm^{-1} persists, albeit with some broadening, indicating overlapping carbonyl groups from both components. Additionally, the P=O and P–O–C stretching bands near 1240 cm^{-1} and 1092 cm^{-1}, respectively, are present but show modifications in intensity and position, further supporting interactions between the extract and phospholipid matrix.[88] These spectral changes indicate that the phospholipid structure remains intact upon encapsulation, with possible hydrogen bonding or electrostatic interactions facilitating the incorporation of the *Moringa* extract (Fig. 3).

4.5. Stability studies

Thermogravimetric analysis was conducted to evaluate the thermal stability of the MO, PhS, and MO-PhS (Fig. 4). The TGA curves exhibited distinct degradation patterns, reflecting the characteristic thermal behavior of each component. The MO curve showed a multi-step degradation process, initiating with a minor weight loss (11.3%) below 150 °C, attributed to the evaporation of residual water or volatile phytoconstituents, followed by a major decomposition event with 45.56% weight loss, occurring between 200 °C and 400 °C. This significant weight loss corresponds to the thermal breakdown of polyphenolic and other thermolabile constituents typically abundant in plant extracts.[89,90]

The phospholipid profile presents in the plain pharmacosomes (PhS) demonstrated relatively better thermal stability, with the primary degradation beginning around 220 °C, with 7.04% weight loss, and extending up to 450 °C (31.32%). This major thermal event is associated with the decomposition of the phosphatidylcholine backbone and fatty acid chains, a finding consistent with previous reports on lecithin-based systems.[91,92] Notably, the MO-loaded pharmacosomes (MO-PhS) exhibited a delayed onset of thermal degradation and a smoother degradation curve compared to its individual components. The primary degradation step for MO-PhS shifted toward higher temperatures (onset 240 °C with 12.8% weight loss) while extended up to 475 °C with 32.8% weight loss, suggesting enhanced thermal stability resulting from successful interaction between MO and the pharmacosomal matrix.

This improvement in thermal resistance may be attributed to the formation of non-covalent interactions such as hydrogen bonding or electrostatic forces between the bioactive constituents of MO and the polar head groups of the phospholipid, particularly the phosphate moieties. Such interactions likely reduce the volatility and mobility of the extract within the lipid matrix, thereby providing a protective effect.[91] Additionally, the more gradual weight loss curve observed in MO-PhS compared to MO suggests a controlled degradation behavior, which may reflect the encapsulation efficiency and the establishment of a stable nanocomplex. Similar stabilization effects have been reported in niosomes and other lipid-based nanocarriers encapsulating polyphenolic compounds.[91,93]

Notably, the nanoformulations were stored at 4 °C for approximately one year, after which FTIR analysis and DLS measurements (size, PDI, and zeta-potential) were repeated,

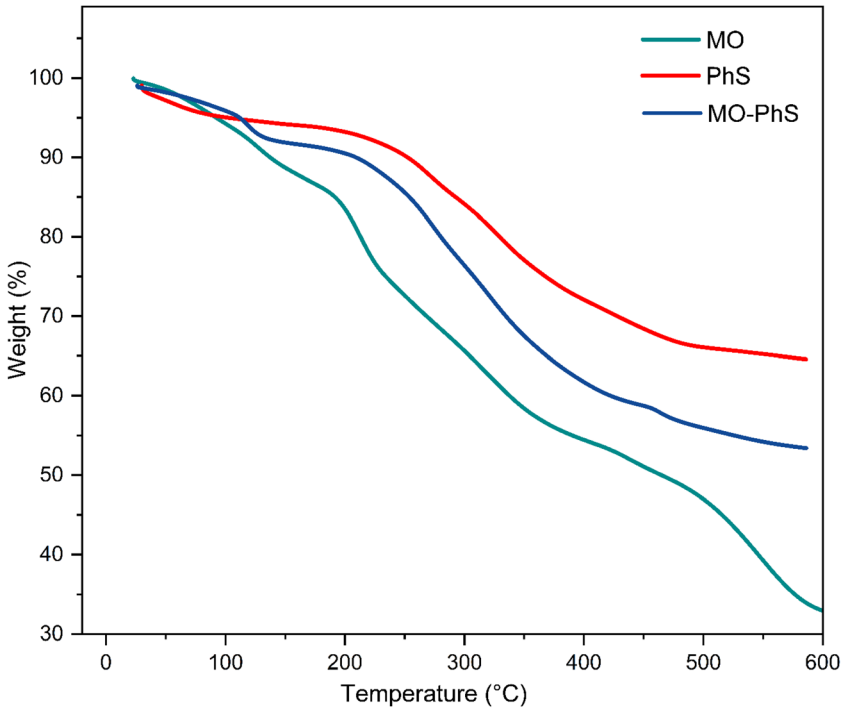

Fig. 4 Thermogravimetric analysis (TGA) curves of *Moringa* extract (MO), plain pharmacosomes (PhS), and *Moringa*-loaded pharmacosomes (MO-PhS). The MO-loaded pharmacosomes exhibited enhanced thermal stability compared to free MO, as evidenced by the delayed onset of major weight loss and smoother degradation profile, but less stability as compared to unloaded pharmacosomes, attributing to the wide range of phytochemicals present in the MO extract, which differ in their polarity nature affecting the structure of the plain pharmacosomes.

and the physical appearance was re-examined. No changes in the FTIR spectra or visible signs of sedimentation or aggregation were observed, indicating good chemical integrity and storage stability of the prepared nanoformulations.

4.6. *In Vitro* biocompatibility assessment on normal human fibroblasts

The biocompatibility of the developed pharmacosomal system was evaluated using normal human fibroblast (hFB) cells to assess the safety profile of the carrier and to determine whether nanoencapsulation confers selectivity toward cancer cells. Cell viability was assessed after exposure to plain PhS, free MO extract, and MO-PhS over the tested concentration range (Fig. 5).

Plain PhS exhibited negligible cytotoxicity toward hFB cells, with cell viability remaining above the accepted biocompatibility threshold across all tested concentrations. This confirms the intrinsic safety of the lecithin–chitosan pharmacosomal matrix and demonstrates that the carrier system itself does not induce nonspecific cytotoxic effects. The excellent biocompatibility observed is consistent with previous reports describing phospholipid-based nanocarriers and chitosan-containing systems as well tolerated by normal cells due to their biomimetic composition and biodegradability.[94,95] In contrast, exposure to the free MO extract resulted in a moderate, concentration-dependent reduction in fibroblast viability, reflecting the presence of bioactive phytochemicals with known biological reactivity. Polyphenolic acids, flavonoids, and fatty acid derivatives identified by GC-MS have previously been reported to exert mild cytostatic or oxidative effects in normal cells at elevated concentrations, particularly when administered in their free form without controlled release. However, this reduction in viability remained substantially lower than that observed in neuroblastoma cells, indicating partial selectivity toward malignant cells. Notably, PhS demonstrated improved biocompatibility compared to the free MO extract, with fibroblast viability consistently higher at equivalent concentrations. This finding suggests that nanoencapsulation effectively modulates the interaction between the phytochemicals and normal cells by controlling their release profile and limiting acute intracellular exposure. The pharmacosomal architecture likely reduces burst-related cytotoxicity while maintaining therapeutic activity in cancer cells, a feature commonly reported for lipid-based nanocarriers encapsulating natural anticancer agents.[94]

The observed selectivity can be attributed to several factors, including the differential endocytic activity between normal fibroblasts and cancer cells, as well as differences in membrane composition and metabolic demand. Cancer cells such as SH-SY5Y neuroblastoma cells exhibit enhanced nanoparticle uptake and heightened sensitivity to redox imbalance, whereas normal fibroblasts possess more robust antioxidant defenses and lower proliferative stress, allowing them to better tolerate controlled phytochemical exposure.[94,95] Overall, these results confirm that the developed MO-PhS possess a favorable safety profile toward normal cells, while retaining strong cytotoxic activity against neuroblastoma cells. This selective behavior

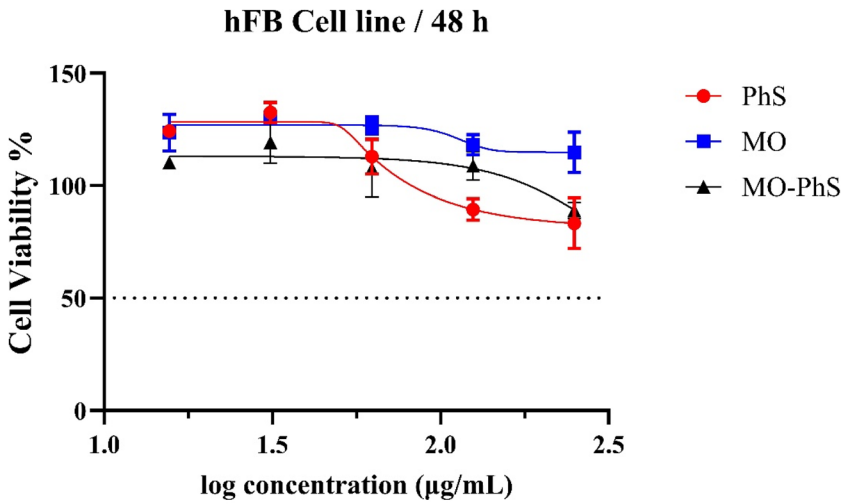

Fig. 5 *In vitro* biocompatibility evaluation of plain PhS, MO extract, and MO-PhS in SH-SY5Y neuroblastoma cells. Cells were exposed to increasing concentrations for 48 h, and cell viability was assessed using the MTT assay. The results demonstrate no significant reduction in cell viability across the tested concentration range, confirming the cytocompatibility and biological safety of the samples. These findings indicate that the observed cytotoxic effects in MO-PhS are attributable exclusively to the encapsulated MO extract rather than the nanocarrier itself. Data represent mean ± SD of three independent experiments ($n = 3$).

supports the suitability of the pharmacosomal system as a cancer-targeted nanocarrier and provides a critical safety foundation for subsequent mechanistic and therapeutic evaluations.

4.7. Cytotoxicity of MO-pharmacosomes in SH-SY5Y cells supported by antioxidant profiling

The cytotoxicity profiles of MO extract, plain PhS, and MO-PhS were assessed on SH-SY5Y neuroblastoma cells using the MTT assay after 48 h of exposure (Fig. 6). The IC_{50} values, derived from the dose–response curves, revealed a significant enhancement in the biological activity of MO upon encapsulation.

The MO extract exhibited moderate antiproliferative activity with an IC_{50} of 695 µg mL^{-1}, aligning with prior studies where polyphenol-rich plant extracts demonstrated tumor-selective, dose-dependent effects on neuroblastoma and other cancer cell lines.[96–98] In contrast, MO-PhS achieved a markedly lower IC_{50} of 67.03 µg mL^{-1}, indicating a roughly 10-fold increase in potency. Plain pharmacosomes, on the other hand, showed negligible cytotoxicity with an IC_{50} exceeding 1000 µg mL^{-1}, thereby confirming the biosafety of the carrier system alone and attributing

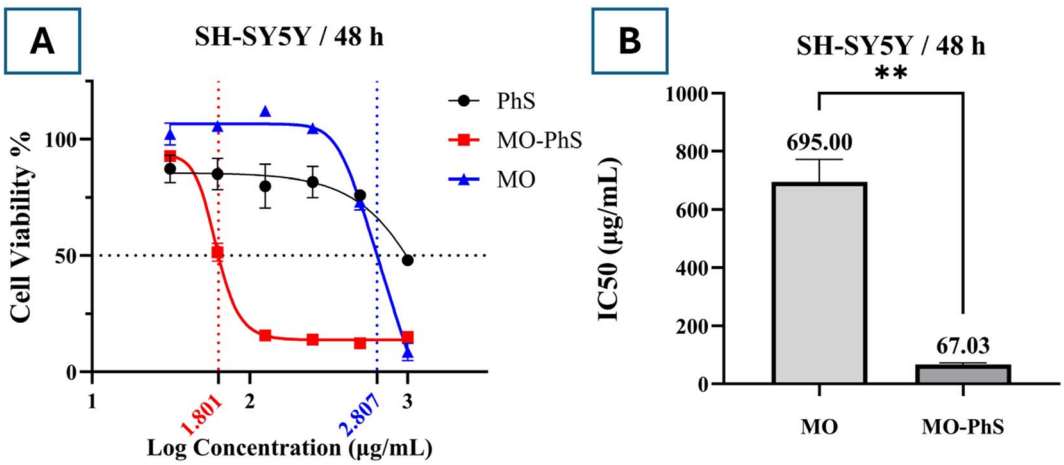

Fig. 6 (A): Cell viability (%) of SH-SY5Y cells treated by *Moringa oleifera* extract (MO), plain pharmacosomes (PhS), and MO-loaded pharmacosomes (MO-PhS), assessed *via* the MTT assay after 48 h. (B) IC_{50} values (µg mL^{-1}) of MO, PhS, and MO-PhS against SH-SY5Y cells. MO-PhS exhibited significantly enhanced cytotoxicity compared to free MO, with an IC_{50} of 67.03 µg mL^{-1}, reflecting improved intracellular delivery and bioactivity. PhS alone showed negligible cytotoxicity (~1000 µg mL^{-1}), confirming the biocompatibility of the nanocarrier. Data represent mean ± SD of three independent experiments ($n = 3$) (*$p < 0.05$; **$p < 0.01$ (0.0074)).

the observed cytotoxicity solely to the encapsulated phytoconstituents.

These findings correlate with the previously reported high EE% (94.52 ± 2.79%), which likely enhanced the bioavailability and intracellular delivery of the MO components. The amphiphilic nature of the phospholipid–chitosan matrix provided a dual-interaction platform capable of encapsulating both hydrophilic and lipophilic compounds, facilitating stable incorporation and controlled release of tumoricidal phytochemicals such as uridine, feruloylquinic acid, flavonoids, and caffeic acid derivatives.[52,54,63,99,100]

In terms of antioxidant capacity, the MO extract demonstrated strong DPPH radical scavenging activity, with inhibition percentages of 65.23%, 68.16%, and 74.71% at concentrations of 15.625, 62.5, and 125 μg mL^{-1}, respectively. This supports the extract's redox-modulating potential and suggests its ability to combat oxidative stress often associated with tumor microenvironments.[101–104]

Recent studies have highlighted the ability of the MO extracts to modulate redox-sensitive signaling pathways and apoptosis-related proteins in neuronal cells. For instance, Barinda *et al.* (2024)[102] showed that MO leaf extract reduced ROS production and downregulated the expression of pro-apoptotic markers such as Bax and caspase-3 while upregulating phosphorylated Akt and CREB in SH-SY5Y neuroblastoma cells exposed to H_2O_2-induced oxidative stress. Although primarily evaluated for neuroprotective purposes, these molecular effects, particularly the modulation of apoptosis and redox homeostasis, also suggest potential relevance in targeting tumor cells.[102] Supporting this, Al-Asmari *et al.* (2015)[36] demonstrated a significant cytotoxic effect of MO leaf and bark extracts against breast (MDA-MB-231) and colorectal (HCT-8) cancer cell lines, inducing apoptosis, cell cycle arrest at the G2/M phase, and inhibiting colony formation and motility.[36] These findings support the potential cytotoxic effect of the MO extract on SH-SY5Y neuroblastoma cells.

The nanoparticulate nature of the system further contributed to enhanced endocytic uptake by SH-SY5Y cells, which display active clathrin-mediated and caveolae-mediated endocytosis, making them particularly responsive to nanoscale formulations. These uptake mechanisms are particularly advantageous when using nanocarriers such as MO-PhS, as clathrin-mediated endocytosis ensures efficient cellular entry, while caveolae-mediated endocytosis facilitates cytoplasmic delivery with minimal lysosomal degradation, a critical feature for effective delivery of cytotoxic payloads.[105–107]

The nanoscale size and surface properties of MO-PhS likely facilitated enhanced membrane penetration and endosomal escape, promoting higher intracellular delivery of phytochemicals. This is crucial for antitumor efficacy, enabling accumulation at the target site, induction of apoptosis, and disruption of proliferative signaling.[108,109]

GC-MS profiling of the MO extract provided further evidence of its anticancer potential by revealing a rich pool of bioactive compounds. Uridine (22.16%) and myo-inositol (4.81%) have shown cytotoxic properties against different tumor tissues, modulating the P13K/Akt pathway (myo-inositol) and inducing ferroptosis (uridine), resulting in suppression of tumor invasiveness.[52,58,59] Polyphenolic acids such as feruloylquinic acid, chlorogenic acid, and caffeic acid derivatives possess potent antioxidant and pro-apoptotic activities in cancer models.[57,64,99,110–119] Nootkatone, a sesquiterpene identified in the extract, has shown cytotoxic and anti-proliferative effects in colorectal cancer cell lines.[71,72] Flavonoid derivatives (29.02%) exhibit broad anticancer properties including ROS scavenging, cell cycle arrest, inhibition of angiogenesis, suppression of key tumor survival pathways, and even induction of apoptosis in tumor cells.[62,63,84,120] Other compounds such as ferulic and fatty acid derivatives further showed promising anticancer activities.[65–70,121,122]

Encapsulation within pharmacosomes also acts as a protective barrier against premature degradation and first-pass metabolism, enhancing the pharmacokinetic and potentially targeting delivery profiles of the loaded phytochemicals. Similar delivery advantages have been reported with other plant-based nanoformulations targeting tumors.[123,124] Importantly, the observed cytotoxicity of MO-PhS at significantly lower doses, alongside the absence of toxicity from the carrier alone, strongly suggests that the effect is tumor-selective rather than nonspecific or cytolytic. Moreover, such nanoformulations have been shown to activate endogenous antioxidant response pathways, particularly nuclear factor erythroid 2-related factor 2 (Nrf2), which governs the expression of various cytoprotective, anti-apoptotic, and anti-tumorigenic genes in cancer systems.[125–128] This may further explain the enhanced bioactivity of MO-PhS compared to the free extract.

Taken together, MO-PhS demonstrated a promising antitumor profile against neuroblastoma cells, combining improved physicochemical properties, enhanced nanoscale uptake, high entrapment of cytotoxic phytochemicals, and a promising cytotoxic profile. The significantly reduced IC_{50} reflects enhanced potency, delivery, and preservation of bioactivity, all of which justify further *in vivo* exploration of this delivery system for neuroblastoma therapy.

4.8. Flow cytometry analysis of cell cycle distribution

The effect of MO and MO-PhS on cell cycle progression in SH-SY5Y neuroblastoma cells is illustrated in Fig. 7. Cells were treated with MO and MO-PhS at their respective IC_{50} concentrations determined by the MTT assay (695 μg mL^{-1} and 67.03 μg mL^{-1}, respectively). Untreated control cells exhibited a typical proliferative profile, with the majority of cells residing in the G0/G1 phase (74.23%), followed by the S phase (24.30%) and a minimal fraction in the G2/M phase (1.47%). Treatment with MO extract resulted in a pronounced redistribution of the cell population, characterized by a reduction in the G0/G1 phase to 62.82%, accompanied by an increase in S phase cells to 31.89% and G2/M phase cells to 5.06%. This shift indicates that MO interferes with cell cycle progression, promoting accumulation of cells in phases associated with DNA synthesis and mitotic preparation. Notably, MO-PhS treatment induced more pronounced cell cycle modulation in terms of S-phase accumulation, with 61.64% of cells in G0/G1, 34.03% in the S phase,

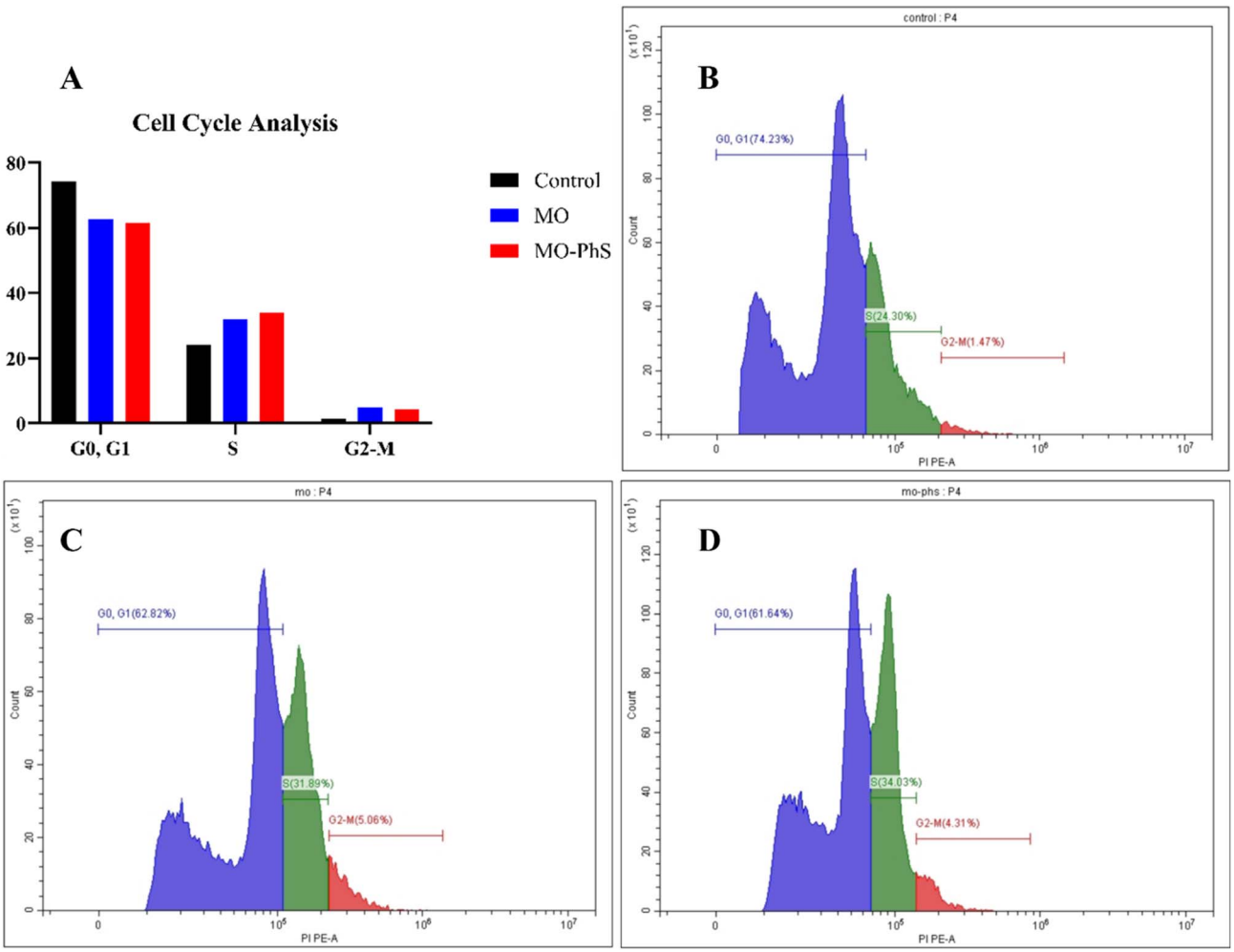

Fig. 7 Flow cytometric analysis of cell cycle distribution in SH-SY5Y neuroblastoma cells following treatment with free MO extract and MO-PhS as compared to control. (A) Cell cycle distribution analysis for control, MO, and MO-PhS; (B) cell cycle distribution for control; (C) cell cycle distribution for MO; (D) cell cycle distribution for MO-PhS.

and 4.31% in the G2/M phase. Importantly, these effects were achieved at a nearly 10-fold lower concentration than that required for the free MO extract, highlighting the superior antiproliferative efficiency of the pharmacosomal formulation.

Despite the similarity in the overall distribution pattern between MO and MO-PhS, the ability of MO-PhS to induce equivalent or stronger S- and G2/M-phase accumulation at a markedly reduced dose highlights the critical role of pharmacosomal encapsulation in enhancing intracellular delivery and bioavailability of MO phytoconstituents. This mirrors the cytotoxicity findings from the MTT assay, where MO-PhS exhibited an approximately 10-fold lower IC_{50} compared to the free extract, confirming that the observed cell cycle effects are dose-efficient and formulation-driven rather than concentration-dependent.

The observed S-phase and G2/M accumulations are indicative of replication stress and checkpoint activation, which are well-established mechanisms leading to growth arrest and apoptosis in cancer cells. Such cell cycle perturbations are commonly associated with DNA damage, inhibition of DNA synthesis, and impaired mitotic progression.[129,130] The enhanced S-phase accumulation observed with MO-PhS suggests a more effective disruption of DNA replication dynamics, consistent with increased intracellular availability of active phytochemicals.

Lipid-based pharmacosomes closely mimic biological membranes, facilitating efficient cellular internalization and sustained intracellular exposure.[131] This enhanced delivery likely amplifies the effects of key MO-derived compounds, such as flavonoids, phenolic acids, and isothiocyanate-related constituents, which are known to interfere with cyclin-dependent kinases, DNA replication machinery, and cell cycle regulatory proteins.[132,133] Importantly, the modulation of cell cycle distribution observed here does not reflect nonspecific cytotoxicity of the carrier system, as plain PhS were shown to be biocompatible in parallel assays. Instead, the data support a mechanism in which pharmacosomal encapsulation potentiates the anticancer activity of the MO extract by improving uptake, stability, and intracellular retention.

Overall, these findings demonstrate that both MO and MO-PhS exert antiproliferative effects in SH-SY5Y neuroblastoma cells through cell cycle arrest; however, MO-PhS achieves these effects at substantially lower concentrations, providing strong mechanistic support for the enhanced cytotoxic efficacy of the nanoformulated system. This dose-efficient cell cycle modulation further validates MO-PhS as a promising nanoplatform for neuroblastoma therapy.

5. Conclusion and future perspectives

This study demonstrates that pharmacosome-based nanocarriers represent an effective strategy to enhance the anticancer potential of *Moringa oleifera* extract against neuroblastoma. The successful incorporation of MO into phospholipid-chitosan pharmacosomes resulted in a stable nanoscale delivery system with high entrapment efficiency, favorable surface properties, and excellent biocompatibility. Importantly, pharmacosomal encapsulation significantly improved the cytotoxic activity of MO against SH-SY5Y neuroblastoma cells (10-fold increase), which was further supported by cell cycle analysis revealing pronounced arrest in S and G2/M phases, indicative of disrupted DNA replication and proliferative signaling. Crucially, these comparable or enhanced cell cycle effects were observed at substantially lower MO concentrations when delivered *via* pharmacosomes, reinforcing the formulation's superior intracellular delivery efficiency and therapeutic potency. Additionally, antioxidant evaluation by the DPPH assay further highlighted the extract's potent free-radical scavenging capacity, which supports its therapeutic potential.

The enhanced biological performance of MO-loaded pharmacosomes can be attributed to improved cellular internalization, sustained intracellular availability of phytochemicals, and strong drug–lipid interactions inherent to pharmacosomal systems. Unlike free extracts, which are often limited by poor solubility and instability, pharmacosomes provide a structurally integrated platform that preserves bioactivity while minimizing nonspecific toxicity, as evidenced by the low cytotoxicity of the plain carrier.

Despite these promising results, several challenges must be addressed to facilitate clinical translation. Scale-up of pharmacosome production requires optimization to ensure batch-to-batch reproducibility and cost-effectiveness, particularly when using complex plant extracts with variable composition. Regulatory approval may also present challenges, as botanical-based nanomedicines must satisfy stringent requirements regarding standardization, safety, and quality control. Furthermore, comprehensive *in vivo* evaluation, pharmacokinetic profiling, and long-term toxicity studies will be essential to validate therapeutic efficacy and safety in clinically relevant models.

Overall, this work provides a strong proof-of-concept for the use of pharmacosome-based nanocarriers to repurpose medicinal plant extracts for cancer therapy. With further optimization and preclinical validation, MO-loaded pharmacosomes may offer a viable and innovative approach for the treatment of neuroblastoma and other brain-related malignancies.

Conflicts of interest

The authors declare no competing interests.

Data availability

The data supporting this article have been included inside the manuscript.

Supplementary information (SI): the GC-MS chromatogram conducted on MO extract. See DOI: https://doi.org/10.1039/d5na00473j.

Acknowledgements

The current work was funded by a grant from the American University in Cairo to Distinguished University Prof. Hassan Azzazy.

References

1 F. Salemi, W. Alam, M. S. Hassani, S. Z. Hashemi, A. A. Jafari, S. M. S. Mirmoeeni, M. Arbab, S. M. R. Mortazavizadeh and H. Khan, Neuroblastoma: Essential genetic pathways and current therapeutic options, *Eur. J. Pharmacol.*, 2022, **926**, 175030, DOI: 10.1016/j.ejphar.2022.175030.

2 K. K. Matthay, J. M. Maris, G. Schleiermacher, A. Nakagawara, C. L. Mackall, L. Diller and W. A. Weiss, Neuroblastoma, *Nat. Rev. Dis. Primers*, 2016, **2**(1), 16078, DOI: 10.1038/nrdp.2016.78.

3 D. J. Newman and G. M. Cragg, Natural Products as Sources of New Drugs over the Nearly Four Decades from 01/1981 to 09/2019, *J. Nat. Prod.*, 2020, **83**(3), 770–803, DOI: 10.1021/acs.jnatprod.9b01285.

4 O. A. A. Alabrahim, J. M. Lababidi, W. Fritzsche and H. M. E.-S. Azzazy, Beyond Aromatherapy: Can Essential Oils Loaded Nanocarriers Revolutionize Cancer Treatment?, *Nanoscale Adv.*, 2024, **6**(22), 5511–5562, DOI: 10.1039/D4NA00678J.

5 G. Stevens, K. Baiyeri and O. Akinnnagbe, Ethno-medicinal and culinary uses of *Moringa* oleifera Lam. in Nigeria, *J. Med. Plants Res.*, 2013, **7**(13), 799–804.

6 A. F. Abdull Razis, M. D. Ibrahim and S. B. Kntayya, Health benefits of *Moringa* oleifera, *Asian Pac. J. Cancer Prev.*, 2014, **15**(20), 8571–8576, DOI: 10.7314/APJCP.2014.15.20.8571.

7 M. Vergara-Jimenez, M. M. Almatrafi and M. L. Fernandez, Bioactive Components in *Moringa* Oleifera Leaves Protect against Chronic Disease, *Antioxidants*, 2017, **6**(4), 91, DOI: 10.3390/antiox6040091.

8 A. Bhattacharya, P. Tiwari, P. K. Sahu and S. Kumar, A review of the phytochemical and pharmacological characteristics of *Moringa* oleifera, *J. Pharm. BioAllied Sci.*, 2018, **10**(4), 181, DOI: 10.4103/jpbs.jpbs_126_18.

9 I. Matic, A. Guidi, M. Kenzo, M. Mattei and A. Galgani, Investigation of medicinal plants traditionally used as dietary supplements: A review on *Moringa* oleifera, *J. Publ. Health Afr.*, 2018, **9**(3), 191–199, DOI: 10.4081/jphia.2018.841.

10 B. K. Paikra and B. Gidwani, Phytochemistry and pharmacology of *Moringa* oleifera Lam, *J. Pharmacopuncture*, 2017, **20**(3), 194, DOI: 10.3831/kpi.2017.20.022.

11 A. Leone, A. Spada, A. Battezzati, A. Schiraldi, J. Aristil and S. Bertoli, *Moringa* oleifera Seeds and Oil: Characteristics and Uses for Human Health, *Int. J. Mol. Sci.*, 2016, **17**(12), 2141, DOI: 10.3390/ijms17122141.

12 M. Nadeem and M. Imran, Promising features of *Moringa* oleifera oil: recent updates and perspectives, *Lipids Health Dis.*, 2016, **15**(1), 212, DOI: 10.1186/s12944-016-0379-0.

13 A. Satish, S. Sairam, F. Ahmed and A. Urooj, *Moringa* oleifera Lam.: Protease activity against blood coagulation cascade, *Pharmacogn. Res.*, 2012, **4**(1), 44–49, DOI: 10.4103/0974-8490.91034.

14 T. Prabsattroo, J. Wattanathorn, S. Iamsaard, P. Somsapt, O. Sritragool, W. Thukhummee and S. Muchimapura, *Moringa* oleifera extract enhances sexual performance in stressed rats, *J. Zhejiang Univ., Sci., B*, 2015, **16**(3), 179–190, DOI: 10.1631/jzus.B1400197.

15 S. Ghimire, L. Subedi, N. Acharya and B. P. Gaire, *Moringa* oleifera: A Tree of Life as a Promising Medicinal Plant for Neurodegenerative Diseases, *J. Agric. Food Chem.*, 2021, **69**(48), 14358–14371, DOI: 10.1021/acs.jafc.1c04581.

16 A. Bhattacharya, P. Tiwari, P. K. Sahu and S. Kumar, A Review of the Phytochemical and Pharmacological Characteristics of Moringa oleifera, *J. Pharm. BioAllied Sci.*, 2018, **10**(4), 181–191, DOI: 10.4103/jpbs.Jpbs_126_18.

17 M. A. Valdez-Solana, V. Y. Mejía-García, A. Téllez-Valencia, G. García-Arenas, J. Salas-Pacheco, J. J. Alba-Romero and E. Sierra-Campos, Nutritional Content and Elemental and Phytochemical Analyses of *Moringa oleifera* Grown in Mexico, *J. Chem.*, 2015, **2015**, 860381, DOI: 10.1155/2015/860381.

18 S. M. Abdulkarim, K. Long, O. M. Lai, S. K. S. Muhammad and H. M. Ghazali, Some physico-chemical properties of *Moringa* oleifera seed oil extracted using solvent and aqueous enzymatic methods, *Food Chem.*, 2005, **93**(2), 253–263, DOI: 10.1016/j.foodchem.2004.09.023.

19 L. Gopalakrishnan, K. Doriya and D. S. Kumar, *Moringa* oleifera: A review on nutritive importance and its medicinal application, *Food Sci. Hum. Wellness*, 2016, **5**(2), 49–56, DOI: 10.1016/j.fshw.2016.04.001.

20 H. P. S. Makkar and K. Becker, Nutrients and antiquality factors in different morphological parts of the *Moringa* oleifera tree, *J. Agric. Sci.*, 1997, **128**(3), 311–322, DOI: 10.1017/S0021859697004292.

21 B. Moyo, P. J. Masika, A. Hugo and V. Muchenje, Nutritional characterization of *Moringa* (*Moringa* oleifera Lam.) leaves, *Afr. J. Biotechnol.*, 2011, **10**(60), 12925–12933, DOI: 10.5897/AJB10.1599.

22 C. Ramachandran, K. V. Peter and P. K. Gopalakrishnan, Drumstick (*Moringa* oleifera): A Multipurpose Indian Vegetable, *Econ. Bot.*, 1980, **34**(3), 276–283.

23 B. Sharma, S. Tripathy, C. R. Kantwa, R. Ghaswa, R. S. Bhadauria and D. R. Pachauri, *Moringa* oleifera: The miracle tree on the Earth, *Int. J. Curr. Microbiol. Appl. Sci.*, 2020, **9**(8), 2623–2632, DOI: 10.20546/ijcmas.2020.908.300.

24 J. D. H. Keatinge, A. W. Ebert, J. A. Hughes, R. Y. Yang, & J. Curaba (2015, November). Seeking to attain the UN's Sustainable Development Goal 2 worldwide: the important role of Moringa oleifera. In *I International Symposium on Moringa 1158* (pp. pp. 1-10).

25 M. Velázquez-Zavala, I. E. Peón-Escalante, R. Zepeda-Bautista and M. A. Jiménez-Arellanes, *Moringa* (*Moringa* oleifera Lam.): potential uses in agriculture, industry and medicine, *Rev. Chapingo Ser. Hortic.*, 2016, **22**(2), 95–116, DOI: 10.5154/r.rchsh.2015.07.018.

26 T. Maraldi, D. Vauzour and C. Angeloni, Dietary Polyphenols and Their Effects on Cell Biochemistry and Pathophysiology 2013, *Oxid. Med. Cell. Longev.*, **2014**, 576363, DOI: 10.1155/2014/576363.

27 A. Ganguly and D. Guha, Alteration of brain monoamines & EEG wave pattern in rat model of Alzheimer's disease & protection by Moringa oleifera, *Indian Journal of medical research*, 2008, **128**(6), 744–751.

28 B. Mahaman, F. Huang, M. Wu, Y. Wang, Z. Wei, J. Bao and X. Wang, Moringa oleifera alleviates homocysteine-induced Alzheimer's disease-like pathology and cognitive impairments, *Journal of Alzheimer's Disease*, 2018, **63**(3), 1141–1159.

29 S. Giacoppo, T. Soundara Rajan, G. R. De Nicola, R. Iori, P. Rollin, P. Bramanti and E. Mazzon, The Isothiocyanate Isolated from *Moringa* oleifera Shows Potent Anti-Inflammatory Activity in the Treatment of Murine Subacute Parkinson's Disease, *Rejuvenation Res*, 2017, **20**(1), 50–63, DOI: 10.1089/rej.2016.1828.

30 A. Giacoppo, T. S. Rajan, G. R. De Nicola, R. Iori, P. Rollin, P. Bramanti and E. Mazzon, The isothiocyanate isolated from Moringa oleifera shows potent anti-inflammatory activity in the treatment of murine subacute Parkinson's disease, *Rejuvenation Research*, 2017, **20**(1), 50–63.

31 B. Singh, P. K. Keshri, V. N. Mishra and S. P. Singh, Moringa oleifera Modulates MPTP-induced Mitochondrial Dysfunction in Parkinson's Mouse Model: An in silico and in vivo Analysis, *Journal of Pharmacology and Pharmacotherapeutics*, 2023, **14**(3), 187–200.

32 W. Kirisattayakul, J. Wattanathorn, T. Tong-Un, S. Muchimapura, P. Wannanon and J. Jittiwat, Cerebroprotective Effect of *Moringa oleifera* against Focal Ischemic Stroke Induced by Middle Cerebral Artery Occlusion, *Oxid. Med. Cell. Longev.*, 2013, 951415, DOI: 10.1155/2013/951415.

33 K. Zeng, Y. Li, W. Yang, Y. Ge, L. Xu, T. Ren, H. Zhang, R. Zhuo, L. Peng, C. Chen, Y. Zhou, Y. Zhao, W. J. Li, X. Jin and L. Yang, *Moringa* oleifera seed extract protects against brain damage in both the acute and delayed

stages of ischemic stroke, *Exp. Gerontol.*, 2019, **122**, 99–108, DOI: 10.1016/j.exger.2019.04.014.

34 S. Sreelatha, A. Jeyachitra and P. R. Padma, Antiproliferation and induction of apoptosis by *Moringa* oleifera leaf extract on human cancer cells, *Food Chem. Toxicol.*, 2011, **49**(6), 1270–1275, DOI: 10.1016/j.fct.2011.03.006.

35 C. Tiloke, A. Phulukdaree and A. A. Chuturgoon, The antiproliferative effect of *Moringa* oleifera crude aqueous leaf extract on cancerous human alveolar epithelial cells, *BMC Compl. Alternative Med.*, 2013, **13**(1), 226, DOI: 10.1186/1472-6882-13-226.

36 A. K. Al-Asmari, S. M. Albalawi, M. T. Athar, A. Q. Khan, H. Al-Shahrani and M. Islam, *Moringa* oleifera as an Anti-Cancer Agent against Breast and Colorectal Cancer Cell Lines, *PLoS One*, 2015, **10**(8), e0135814, DOI: 10.1371/journal.pone.0135814.

37 F. Alhakmani, S. Kumar and S. A. Khan, Estimation of total phenolic content, in–vitro antioxidant and anti–inflammatory activity of flowers of *Moringa* oleifera, *Asian Pac. J. Trop. Biomed.*, 2013, **3**(8), 623–627, DOI: 10.1016/S2221-1691(13)60126-4.

38 A. Leone, A. Spada, A. Battezzati, A. Schiraldi, J. Aristil and S. Bertoli, Cultivation, Genetic, Ethnopharmacology, Phytochemistry and Pharmacology of *Moringa* oleifera Leaves: An Overview, *Int. J. Mol. Sci.*, 2015, **16**(6), 12791–12835, DOI: 10.3390/ijms160612791.

39 A. Semalty, S. Mona, R. B. Singh, S. Devendra and M. S. M. Rawat, Pharmacosomes: the lipid-based new drug delivery system, *Expet Opin. Drug Deliv.*, 2009, **6**(6), 599–612, DOI: 10.1517/17425240902967607.

40 A. Semalty, M. Semalty, D. Singh and M. Rawat, Development and physicochemical evaluation of pharmacosomes of diclofenac, *Acta Pharm.*, 2009, **59**(3), 335–344, DOI: 10.2478/v10007-009-0023-x.

41 A. Pandita and P. Sharma, Pharmacosomes: an emerging novel vesicular drug delivery system for poorly soluble synthetic and herbal drugs, *ISRN Pharm.*, 2013, **2013**, 348186, DOI: 10.1155/2013/348186.

42 B. Supraja and S. Mulangi, An updated review on pharmacosomes, a vesicular drug delivery system, *J. Drug Deliv. Therapeut.*, 2019, **9**(1-s), 393–402, DOI: 10.22270/jddt.v9i1-s.2234.

43 A. Sharma and U. S. Sharma, Liposomes in drug delivery: Progress and limitations, *Int. J. Pharm.*, 1997, **154**(2), 123–140, DOI: 10.1016/S0378-5173(97)00135-X.

44 H. Perumalsamy, S. R. Balusamy, J. Sukweenadhi, S. Nag, D. MubarakAli, M. El-Agamy Farh, H. Vijay and S. Rahimi, A comprehensive review on *Moringa* oleifera nanoparticles: importance of polyphenols in nanoparticle synthesis, nanoparticle efficacy and their applications, *J. Nanobiotechnol.*, 2024, **22**(1), 71, DOI: 10.1186/s12951-024-02332-8.

45 Y. Kotha, A. G. Kandhula and K. Janapareddi, Development and characterization of levodopa loaded pharmacosomes for brain targeting via intranasal route: Pharmacodynamic evaluation in rats, *J. Young Pharm.*, 2020, **12**(2s), s56, DOI: 10.5530/jyp.2020.12s.47.

46 W. C. Samms *Catecholamine Disturbance and SH-Sy5y Cell Toxicity of Halogenated 3-amino-2 Phenylpropenes*. Wichita State University, College of Liberal Arts and Sciences, Department, 2009.

47 S. Vijayakumar, V. Bhuvaneshwari and A. Sumathi, Antioxidant and anticancer potential of methanolic leaf extract of Moringa concanensis Nimmo against human breast cancer cell line MCF-7, *International Journal of Pharmacognosy and Phytochemical Research*, 2017, **9**(6), 750–754.

48 J. M. Halket and V. G. Zaikin, Derivatization in Mass Spectrometry—1. Silylation, *Eur. J. Mass Spectrom.*, 2003, **9**(1), 1–21, DOI: 10.1255/ejms.527.

49 J. Rohloff, Analysis of Phenolic and Cyclic Compounds in Plants Using Derivatization Techniques in Combination with GC-MS-Based Metabolite Profiling, *Molecules*, 2015, **20**(2), 3431–3462, DOI: 10.3390/molecules20023431.

50 J. He, S. Ouyang, X. Chen and C. Xie, Copper-Containing Mesoporous Bioactive Glass Nanoparticles: A Novel Radiosensitizer for Nonsmall Cell Lung Cancer, *Adv. NanoBiomed Res.*, 2025, **5**(12), 2500084, DOI: 10.1002/anbr.202500084.

51 M. T. Abo-Elfadl and A. M. Mansour, Cytotoxic properties of fac-Re(CO)3 complexes with quinoline coligands: Insights on the mode of cell death and DNA fragmentation, *Inorg. Chim. Acta*, 2023, **553**, 121521, DOI: 10.1016/j.ica.2023.121521.

52 L. Zi, W. Ma, L. Zhang, B. Qiao, Z. Qiu, J. Xu, J. Zhang, Y. Ye, Y. Yang, K. Dong, C. Chen, W. Wang and Q. Zhao, Uridine Inhibits Hepatocellular Carcinoma Cell Development by Inducing Ferroptosis, *J. Clin. Med.*, 2023, **12**(10), 3552, DOI: 10.3390/jcm12103552.

53 Z. Wu, Y. Zhu, W. Liu, B. Balasubramanian, X. Xu, J. Yao and X. Lei, Ferroptosis in Liver Disease: Natural Active Compounds and Therapeutic Implications, *Antioxidants*, 2024, **13**(3), 352, DOI: 10.3390/antiox13030352.

54 J. Wang, S. Xu, W. Lv, F. Shi, S. Mei, A. Shan, J. Xu and Y. Yang, Uridine phosphorylase 1 is a novel immune-related target and predicts worse survival in brain glioma, *Cancer Med.*, 2020, **9**(16), 5940–5947, DOI: 10.1002/cam4.3251.

55 Y. Yang, Y. Ye, Y. Deng and L. Gao, Uridine and its role in metabolic diseases, tumors, and neurodegenerative diseases, *Front. Physiol.*, 2024, **15**, 1360891, DOI: 10.3389/fphys.2024.1360891.

56 J. K. Wang, C. W. Phan, S.-C. Cheah and V. Sabaratnam, Uridine From a Standardized Aqueous Extract of Giant Oyster Mushroom, Pleurotus giganteus Inhibits Amyloid β (Aβ)-Induced Cytotoxicity in Human Neuroblastoma SH-SY5Y Cells, *Proc. Natl. Acad. Sci., India, Sect. B*, 2022, **92**(3), 575–579, DOI: 10.1007/s40011-021-01339-7.

57 J. Zhou, F. Zhang, J. Chen, S. Zhang and H. Wang, Chlorogenic Acid Inhibits Human Glioma U373 Cell Progression via Regulating the SRC/MAPKs Signal Pathway: Based on Network Pharmacology Analysis, *Drug*

Des., Dev. Ther., 2021, **15**, 1369–1383, DOI: 10.2147/dddt.S296862.

58 M. Bizzarri, S. Dinicola, A. Bevilacqua and A. Cucina, Broad Spectrum Anticancer Activity of myo-Inositol and Inositol Hexakisphosphate, *Int. J. Endocrinol.*, 2016, **2016**, 5616807, DOI: 10.1155/2016/5616807.

59 M. Mormando, G. Puliani, M. Bianchini, R. Lauretta and M. Appetecchia, The Role of Inositols in Endocrine and Neuroendocrine Tumors, *Biomolecules*, 2024, **14**(8), 1004, DOI: 10.3390/biom14081004.

60 J. Lee, Q. N. Nguyen, J. Y. Park, S. Lee, G. S. Hwang, N. Yamabe, S. Choi and K. S. Kang, Protective Effect of Shikimic Acid against Cisplatin-Induced Renal Injury: In Vitro and In Vivo Studies, *Plants*, 2020, **9**(12), 1681, DOI: 10.3390/plants9121681.

61 K. Manna, A. Khan, D. Kr Das, S. Bandhu Kesh, U. Das, S. Ghosh, R. Sharma Dey, K. Das Saha, A. Chakraborty, S. Chattopadhyay, S. Dey and D. Chattopadhyay, Protective effect of coconut water concentrate and its active component shikimic acid against hydroperoxide mediated oxidative stress through suppression of NF-κB and activation of Nrf2 pathway, *J. Ethnopharmacol.*, 2014, **155**(1), 132–146, DOI: 10.1016/j.jep.2014.04.046.

62 V. Sharma, C. Joseph, S. Ghosh, A. Agarwal, M. K. Mishra and E. Sen, Kaempferol induces apoptosis in glioblastoma cells through oxidative stress, *Mol. Cancer Ther.*, 2007, **6**(9), 2544–2553, DOI: 10.1158/1535-7163.Mct-06-0788.

63 D. M. Kopustinskiene, V. Jakstas, A. Savickas and J. Bernatoniene, Flavonoids as Anticancer Agents, *Nutrients*, 2020, **12**(2), 457, DOI: 10.3390/nu12020457.

64 S. Di Giacomo, E. Percaccio, M. Gullì, A. Romano, A. Vitalone, G. Mazzanti, S. Gaetani and A. Di Sotto, Recent Advances in the Neuroprotective Properties of Ferulic Acid in Alzheimer's Disease: A Narrative Review, *Nutrients*, 2022, **14**(18), 3709, DOI: 10.3390/nu14183709.

65 G. W. Yang, J. S. Jiang and W. Q. Lu, Ferulic Acid Exerts Anti-Angiogenic and Anti-Tumor Activity by Targeting Fibroblast Growth Factor Receptor 1-Mediated Angiogenesis, *Int. J. Mol. Sci.*, 2015, **16**(10), 24011–24031, DOI: 10.3390/ijms161024011.

66 A. Markowska, J. Markowska, J. Stanisławiak-Rudowicz, K. Kozak, O. K. Roubinek and M. Jasińska, The Role of Ferulic Acid in Selected Malignant Neoplasms, *Molecules*, 2025, **30**(5), 1018, DOI: 10.3390/molecules30051018.

67 X. Bao, W. Li, R. Jia, D. Meng, H. Zhang and L. Xia, Molecular mechanism of ferulic acid and its derivatives in tumor progression, *Pharmacol. Rep.*, 2023, **75**(4), 891–906, DOI: 10.1007/s43440-023-00494-0.

68 R. I. El-Gogary, M. Nasr, L. A. Rahsed and M. A. Hamzawy, Ferulic acid nanocapsules as a promising treatment modality for colorectal cancer: Preparation and in vitro/in vivo appraisal, *Life Sci.*, 2022, **298**, 120500, DOI: 10.1016/j.lfs.2022.120500.

69 H. Singh Tuli, A. Kumar, S. Ramniwas, R. Coudhary, D. Aggarwal, M. Kumar, U. Sharma, N. Chaturvedi Parashar, S. Haque and K. Sak, Ferulic Acid: A Natural Phenol That Inhibits Neoplastic Events through Modulation of Oncogenic Signaling, *Molecules*, 2022, **27**(21), 7653, DOI: 10.3390/molecules27217653.

70 N. Kumar, S. Kumar, S. Abbat, K. Nikhil, S. M. Sondhi, P. V. Bharatam, P. Roy and V. Pruthi, Ferulic acid amide derivatives as anticancer and antioxidant agents: synthesis, thermal, biological and computational studies, *Med. Chem. Res.*, 2016, **25**(6), 1175–1192, DOI: 10.1007/s00044-016-1562-6.

71 E. Yoo, J. Lee, P. Lertpatipanpong, J. Ryu, C. T. Kim, E. Y. Park and S. J. Baek, Anti-proliferative activity of A. Oxyphylla and its bioactive constituent nootkatone in colorectal cancer cells, *BMC Cancer*, 2020, **20**(1), 881, DOI: 10.1186/s12885-020-07379-y.

72 L. V. M. Hung, J. Y. Moon, J.-y. Ryu and S. K. Cho, Nootkatone, an AMPK activator derived from grapefruit, inhibits KRAS downstream pathway and sensitizes non-small-cell lung cancer A549 cells to adriamycin, *Phytomedicine*, 2019, **63**, 153000, DOI: 10.1016/j.phymed.2019.153000.

73 F. Natali, L. Siculella, S. Salvati and G. V. Gnoni, Oleic acid is a potent inhibitor of fatty acid and cholesterol synthesis in C6 glioma cells, *J. Lipid Res.*, 2007, **48**(9), 1966–1975, DOI: 10.1194/jlr.M700051-JLR200.

74 S. Peretz Damari, D. Shamrakov, M. Varenik, E. Koren, E. Nativ-Roth, Y. Barenholz and O. Regev, Practical aspects in size and morphology characterization of drug-loaded nano-liposomes, *Int. J. Pharm.*, 2018, **547**(1), 648–655, DOI: 10.1016/j.ijpharm.2018.06.037.

75 M. Ghezzi, S. Pescina, C. Padula, P. Santi, E. Del Favero, L. Cantù and S. Nicoli, Polymeric micelles in drug delivery: An insight of the techniques for their characterization and assessment in biorelevant conditions, *J. Controlled Release*, 2021, **332**, 312–336, DOI: 10.1016/j.jconrel.2021.02.031.

76 N. Petersen, M. Girard, A. Riedinger and O. Valsson, The Crucial Role of Solvation Forces in the Steric Stabilization of Nanoplatelets, *Nano Lett.*, 2022, **22**(24), 9847–9853, DOI: 10.1021/acs.nanolett.2c02848.

77 O. Gustafsson, S. Gustafsson, L. Manukyan and A. Mihranyan, Significance of Brownian Motion for Nanoparticle and Virus Capture in Nanocellulose-Based Filter Paper, *Membranes*, 2018, **8**(4), 90, DOI: 10.3390/membranes8040090.

78 M. Danaei, M. Dehghankhold, S. Ataei, F. Hasanzadeh Davarani, R. Javanmard, A. Dokhani, S. Khorasani and M. R. Mozafari, Impact of Particle Size and Polydispersity Index on the Clinical Applications of Lipidic Nanocarrier Systems, *Pharmaceutics*, 2018, **10**(2), 57, DOI: 10.3390/pharmaceutics10020057.

79 L. Zhang, F. Gu, J. Chan, A. Wang, R. Langer and O. Farokhzad, Nanoparticles in Medicine: Therapeutic Applications and Developments, *Clin. Pharmacol. Therapeut.*, 2008, **83**(5), 761–769, DOI: 10.1038/sj.clpt.6100400.

80 O. A. A. Alabrahim and H. M. E.-S. Azzazy, Antimicrobial Activities of Pistacia lentiscus Essential Oils

Nanoencapsulated into Hydroxypropyl-beta-cyclodextrins, *ACS Omega*, 2024, **9**(11), 12622–12634, DOI: 10.1021/acsomega.3c07413.

81 Y. Zhang, H. F. Chan and K. W. Leong, Advanced materials and processing for drug delivery: The past and the future, *Adv. Drug Delivery Rev.*, 2013, **65**(1), 104–120, DOI: 10.1016/j.addr.2012.10.003.

82 C. Saraiva, C. Praça, R. Ferreira, T. Santos, L. Ferreira and L. Bernardino, Nanoparticle-mediated brain drug delivery: Overcoming blood–brain barrier to treat neurodegenerative diseases, *J. Controlled Release*, 2016, **235**, 34–47, DOI: 10.1016/j.jconrel.2016.05.044.

83 J. Kreuter, Drug delivery to the central nervous system by polymeric nanoparticles: What do we know?, *Adv. Drug Delivery Rev.*, 2014, **71**, 2–14, DOI: 10.1016/j.addr.2013.08.008.

84 M. Huang, E. Su, F. Zheng and C. Tan, Encapsulation of flavonoids in liposomal delivery systems: the case of quercetin, kaempferol and luteolin, *Food Funct.*, 2017, **8**(9), 3198–3208, DOI: 10.1039/C7FO00508C.

85 P. Sengupta, A. Bose and K. Sen, Liposomal Encapsulation of Phenolic Compounds for Augmentation of Bio-Efficacy: A Review, *ChemistrySelect*, 2021, **6**(38), 10447–10463, DOI: 10.1002/slct.202101821.

86 S. Khalid, M. Arshad, S. Mahmood, F. Siddique, U. Roobab, M. M. A. N. Ranjha and J. M. Lorenzo, Extraction and Quantification of *Moringa* oleifera Leaf Powder Extracts by HPLC and FTIR, *Food Anal. Methods*, 2023, **16**(4), 787–797, DOI: 10.1007/s12161-023-02470-z.

87 R. Joshi, R. Sathasivam, S. U. Park, H. Lee, M. S. Kim, I. Baek and B.-K. Cho, Application of Fourier Transform Infrared Spectroscopy and Multivariate Analysis Methods for the Non-Destructive Evaluation of Phenolics Compounds in *Moringa* Powder, *Agriculture*, 2022, **12**(1), 10, DOI: 10.3390/agriculture12010010.

88 S. Nandhini and K. Ilango, Development and characterization of a nano-drug delivery system containing vasaka phospholipid complex to improve bioavailability using quality by design approach, *Res. Pharm. Sci.*, 2021, **16**(1), 103–117, DOI: 10.4103/1735-5362.305193.

89 N. N. Tafu and V. A. Jideani, Characterization of Novel Solid Dispersions of *Moringa* oleifera Leaf Powder Using Thermo-Analytical Techniques, *Processes*, 2021, **9**(12), 2230, DOI: 10.3390/pr9122230.

90 T. T. George, A. B. Oyenihi, F. Rautenbach and A. O. Obilana, Characterization of *Moringa* oleifera Leaf Powder Extract Encapsulated in Maltodextrin and/or Gum Arabic Coatings, *Foods*, 2021, **10**(12), 3044, DOI: 10.3390/foods10123044.

91 S. A. Ghumman, A. Ijaz, S. Noreen, A. Aslam, R. Kausar, A. Irfan, S. Latif, G. A. Shazly, P. A. Shah, M. Rana, A. Aslam, M. Altaf, K. Kotwica-Mojzych and Y. A. Bin Jardan, Formulation and Characterization of Curcumin Niosomes: Antioxidant and Cytotoxicity Studies, *Pharmaceuticals*, 2023, **16**(10), 1406, DOI: 10.3390/ph16101406.

92 M. S. de Lima, L. A. Rocha, E. F. Molina, B. L. Caetano, L. Marçal, C. Mello, K. J. Ciuffi, P. S. Calefi and E. J. Nassar, Thermoanalysis of soybean oil extracted by two methods, *Quim. Nova*, 2008, **31**, 527–529.

93 J. Naktiyok, H. Bayrakçeken, A. K. Özer and M. Ş. Gülaboğlu, Kinetics of thermal decomposition of phospholipids obtained from phosphate rock, *Fuel Process. Technol.*, 2013, **116**, 158–164, DOI: 10.1016/j.fuproc.2013.05.007.

94 M. S. Valencia, M. F. D. Silva Júnior, F. H. Xavier-Júnior, B. D. O. Veras, P. B. S. D. Albuquerque, E. F. D. O. Borba, T. G. D. Silva, V. L. Xavier, M. P. D. Souza and M. D. G. Carneiro-da-Cunha, Characterization of curcumin-loaded lecithin-chitosan bioactive nanoparticles, *Carbohydr. Polym. Technol. Appl.*, 2021, **2**, 100119, DOI: 10.1016/j.carpta.2021.100119.

95 L. H. Zoe, S. R. David and R. Rajabalaya, Chitosan nanoparticle toxicity: A comprehensive literature review of in vivo and in vitro assessments for medical applications, *Toxicol Rep*, 2023, **11**, 83–106, DOI: 10.1016/j.toxrep.2023.06.012.

96 P. O. Abolarin, A. Amin, A. B. Nafiu, O. M. Ogundele and B. V. Owoyele, Optimization of Parkinson's disease therapy with plant extracts and nutrition's evolving roles, *IBRO Neurosci. Rep.*, 2024, **17**, 1–12, DOI: 10.1016/j.ibneur.2024.05.011.

97 P. Arulselvan, M. T. Fard, W. S. Tan, S. Gothai, S. Fakurazi, M. E. Norhaizan and S. S. Kumar, Role of Antioxidants and Natural Products in Inflammation, *Oxid. Med. Cell. Longev.*, 2016, **2016**(1), 5276130, DOI: 10.1155/2016/5276130.

98 A. Kafoud, Z. Salahuddin, R. S. Ibrahim, R. Al-Janahi, A. Mazurakova, P. Kubatka and D. Büsselberg, Potential Treatment Options for Neuroblastoma with Polyphenols through Anti-Proliferative and Apoptotic Mechanisms, *Biomolecules*, 2023, **13**(3), 563, DOI: 10.3390/biom13030563.

99 X. Ao, J. Yan, S. Liu, S. Chen, L. Zou, Y. Yang, L. He, S. Li, A. Liu and K. Zhao, Extraction, isolation and identification of four phenolic compounds from Pleioblastus amarus shoots and their antioxidant and anti-inflammatory properties in vitro, *Food Chem.*, 2022, **374**, 131743, DOI: 10.1016/j.foodchem.2021.131743.

100 A. Murugesan, S. Holmstedt, K. C. Brown, A. Koivuporras, A. S. Macedo, N. Nguyen, P. Fonte, P. Rijo, O. Yli-Harja, N. R. Candeias and M. Kandhavelu, Design and synthesis of novel quinic acid derivatives: in vitro cytotoxicity and anticancer effect on glioblastoma, *Future Med. Chem.*, 2020, **12**(21), 1891–1910, DOI: 10.4155/fmc-2020-0194.

101 C. J. Dillard and J. B. German, Phytochemicals: nutraceuticals and human health, *J. Sci. Food Agric.*, 2000, **80**(12), 1744–1756, DOI: 10.1002/1097-0010(20000915)80:12<1744::AID-JSFA725>3.0.CO;2-W.

102 A. J. Barinda, W. Arozal, H. Hardi, Y. R. Dewi, M. S. Safutra and H. J. Lee, Water Extracts of *Moringa* oleifera Leaves Alter Oxidative Stress–Induced Neurotoxicity in Human Neuroblastoma SH-SY5Y Cells, *Sci. World J.*, 2024, **2024**(1), 7652217, DOI: 10.1155/2024/7652217.

103 C. Gorrini, I. S. Harris and T. W. Mak, Modulation of oxidative stress as an anticancer strategy, *Nat. Rev. Drug Discovery*, 2013, **12**(12), 931–947, DOI: 10.1038/nrd4002.
104 V. Sosa, T. Moliné, R. Somoza, R. Paciucci, H. Kondoh and M. E. Lleonart, Oxidative stress and cancer: An overview, *Ageing Res. Rev.*, 2013, **12**(1), 376–390, DOI: 10.1016/j.arr.2012.10.004.
105 J. Rejman, V. Oberle, I. S. Zuhorn and D. Hoekstra, Size-dependent internalization of particles via the pathways of clathrin- and caveolae-mediated endocytosis, *Biochem. J.*, 2004, **377**(Pt 1), 159–169, DOI: 10.1042/bj20031253.
106 A. K. Varkouhi, M. Scholte, G. Storm and H. J. Haisma, Endosomal escape pathways for delivery of biologicals, *J. Controlled Release*, 2011, **151**(3), 220–228, DOI: 10.1016/j.jconrel.2010.11.004.
107 S. A. Chime and M. A. Momoh, PEGylated Nanocarriers for Drug Delivery Applications. in *PEGylated Nanocarriers in Medicine and Pharmacy*, ed. R. K. Tekade, N. K. Jain, Springer Nature Singapore, Singapore, 2025, pp 107–136.
108 D. Zhao, W. Tao, S. Li, Y. Chen, Y. Sun, Z. He, B. Sun and J. Sun, Apoptotic body-mediated intercellular delivery for enhanced drug penetration and whole tumor destruction, *Sci. Adv.*, 2021, **7**(16), eabg0880, DOI: 10.1126/sciadv.abg0880.
109 S. A. Smith, L. I. Selby, A. P. R. Johnston and G. K. Such, The Endosomal Escape of Nanoparticles: Toward More Efficient Cellular Delivery, *Bioconjugate Chem.*, 2019, **30**(2), 263–272, DOI: 10.1021/acs.bioconjchem.8b00732.
110 S. Huang, L. L. Wang, N. N. Xue, C. Li, H. H. Guo, T. K. Ren, Y. Zhan, W. B. Li, J. Zhang, X. G. Chen, Y. X. Han, J. L. Zhang and J. D. Jiang, Chlorogenic acid effectively treats cancers through induction of cancer cell differentiation, *Theranostics*, 2019, **9**(23), 6745–6763, DOI: 10.7150/thno.34674.
111 T. Murai and S. Matsuda, The Chemopreventive Effects of Chlorogenic Acids, Phenolic Compounds in Coffee, against Inflammation, Cancer, and Neurological Diseases, *Molecules*, 2023, **28**(5), 2381, DOI: 10.3390/molecules28052381.
112 G. Kalló, B. Kunkli, Z. Győri, Z. Szilvássy, É. Csősz and J. Tőzsér, Compounds with Antiviral, Anti-Inflammatory and Anticancer Activity Identified in Wine from Hungary's Tokaj Region via High Resolution Mass Spectrometry and Bioinformatics Analyses, *Int. J. Mol. Sci.*, 2020, **21**(24), 9547, DOI: 10.3390/ijms21249547.
113 C. Menozzi-Smarrito, C. C. Wong, W. Meinl, H. Glatt, R. Fumeaux, C. Munari, F. Robert, G. Williamson and D. Barron, First Chemical Synthesis and in Vitro Characterization of the Potential Human Metabolites 5-O-Feruloylquinic Acid 4′-Sulfate and 4′-O-Glucuronide, *J. Agric. Food Chem.*, 2011, **59**(10), 5671–5676, DOI: 10.1021/jf200272m.
114 K. Sidoryk, A. Jaromin, N. Filipczak, P. Cmoch and M. Cybulski, Synthesis and Antioxidant Activity of Caffeic Acid Derivatives, *Molecules*, 2018, **23**(9), 2199, DOI: 10.3390/molecules23092199.
115 E. P. Chiang, S. Y. Tsai, Y. H. Kuo, M. H. Pai, H. L. Chiu, R. L. Rodriguez and F. Y. Tang, Caffeic acid derivatives inhibit the growth of colon cancer: involvement of the PI3-K/Akt and AMPK signaling pathways, *PLoS One*, 2014, **9**(6), e99631, DOI: 10.1371/journal.pone.0099631.
116 M. Lukáč, L. Slobodníková, M. Mrva, A. Dušeková, M. Garajová, M. Kello, D. Šebová, M. Pisárčik, M. Kojnok, A. Vrták, E. Kurin and S. Bittner Fialová, Caffeic Acid Phosphanium Derivatives: Potential Selective Antitumor, Antimicrobial and Antiprotozoal Agents, *Int. J. Mol. Sci.*, 2024, **25**(2), 1200, DOI: 10.3390/ijms25021200.
117 M. Alam, S. Ahmed, A. M. Elasbali, M. Adnan, S. Alam, M. I. Hassan and V. R. Pasupuleti, Therapeutic Implications of Caffeic Acid in Cancer and Neurological Diseases, *Front. Oncol.*, 2022, **12**, 860508, DOI: 10.3389/fonc.2022.860508.
118 S. Mirzaei, M. H. Gholami, A. Zabolian, H. Saleki, M. V. Farahani, S. Hamzehlou, F. B. Far, S. O. Sharifzadeh, S. Samarghandian, H. Khan, A. R. Aref, M. Ashrafizadeh, A. Zarrabi and G. Sethi, Caffeic acid and its derivatives as potential modulators of oncogenic molecular pathways: New hope in the fight against cancer, *Pharmacol. Res.*, 2021, **171**, 105759, DOI: 10.1016/j.phrs.2021.105759.
119 M. Alam, G. M. Ashraf, K. Sheikh, A. Khan, S. Ali, M. M. Ansari, M. Adnan, V. R. Pasupuleti and M. I. Hassan, Potential Therapeutic Implications of Caffeic Acid in Cancer Signaling: Past, Present, and Future, *Front. Pharmacol*, 2022, **13**, 2022, DOI: 10.3389/fphar.2022.845871.
120 D. Vauzour, K. Vafeiadou, A. Rodriguez-Mateos, C. Rendeiro and J. P. Spencer, The neuroprotective potential of flavonoids: a multiplicity of effects, *Gene Nutr.*, 2008, **3**(3–4), 115–126, DOI: 10.1007/s12263-008-0091-4.
121 L. Jiang, W. Wang, Q. He, Y. Wu, Z. Lu, J. Sun, Z. Liu, Y. Shao and A. Wang, Oleic acid induces apoptosis and autophagy in the treatment of Tongue Squamous cell carcinomas, *Sci. Rep.*, 2017, **7**(1), 11277, DOI: 10.1038/s41598-017-11842-5.
122 F. Giulitti, S. Petrungaro, S. Mandatori, L. Tomaipitinca, V. de Franchis, A. D'Amore, A. Filippini, E. Gaudio, E. Ziparo and C. Giampietri, Anti-tumor Effect of Oleic Acid in Hepatocellular Carcinoma Cell Lines via Autophagy Reduction, *Front. Cell Dev. Biol.*, 2021, **9**, 2021, DOI: 10.3389/fcell.2021.629182.
123 T. Andreani, R. Cheng, K. Elbadri, C. Ferro, T. Menezes, M. R. dos Santos, C. M. Pereira and H. A. Santos, Natural compounds-based nanomedicines for cancer treatment: Future directions and challenges, *Drug Deliv. Transl. Res.*, 2024, **14**(10), 2845–2916, DOI: 10.1007/s13346-024-01649-z.
124 A. S. Sedeky, I. A. Khalil, A. Hefnawy and I. M. El-Sherbiny, Development of core-shell nanocarrier system for augmenting piperine cytotoxic activity against human brain cancer cell line, *Eur. J. Pharm. Sci.*, 2018, **118**, 103–112, DOI: 10.1016/j.ejps.2018.03.030.

125 A. P. Kamath, P. G. Nayak, J. John, S. Mutalik, A. K. Balaraman and N. Krishnadas, Revolutionizing neurotherapeutics: Nanocarriers unveiling the potential of phytochemicals in Alzheimer's disease, *Neuropharmacology*, 2024, **259**, 110096, DOI: 10.1016/j.neuropharm.2024.110096.

126 B. Salehi, L. Machin, L. Monzote, J. Sharifi-Rad, S. M. Ezzat, M. A. Salem, R. M. Merghany, N. M. El Mahdy, C. S. Kılıç, O. Sytar, M. Sharifi-Rad, F. Sharopov, N. Martins, M. Martorell and W. C. Cho, Therapeutic Potential of Quercetin: New Insights and Perspectives for Human Health, *ACS Omega*, 2020, **5**(20), 11849–11872, DOI: 10.1021/acsomega.0c01818.

127 C. H. Hsieh, H. C. Hsieh, F. S. Shih, P. W. Wang, L. X. Yang, D. B. Shieh and Y. C. Wang, An innovative NRF2 nano-modulator induces lung cancer ferroptosis and elicits an immunostimulatory tumor microenvironment, *Theranostics*, 2021, **11**(14), 7072–7091, DOI: 10.7150/thno.57803.

128 S. Saha, N. Sachivkina, A. Karamyan, E. Novikova and T. Chubenko, Advances in Nrf2 Signaling Pathway by Targeted Nanostructured-Based Drug Delivery Systems, *Biomedicines*, 2024, **12**(2), 403, DOI: 10.3390/biomedicines12020403.

129 H. K. Matthews, C. Bertoli and R. A. M. de Bruin, Cell cycle control in cancer, *Nat. Rev. Mol. Cell Biol.*, 2022, **23**(1), 74–88, DOI: 10.1038/s41580-021-00404-3.

130 A. da Costa, D. Chowdhury, G. I. Shapiro, A. D. D'Andrea and P. A. Konstantinopoulos, Targeting replication stress in cancer therapy, *Nat. Rev. Drug Discov.*, 2023, **22**(1), 38–58, DOI: 10.1038/s41573-022-00558-5.

131 D. Suhag, S. Kaushik and V. B. Taxak, Drug Delivery via Lipid-Based Nanocarriers, in *Handbook of Biomaterials for Medical Applications*, Springer, 2024, Vol. 1, pp. 297–328.

132 M. Sodvadiya, H. Patel, A. Mishra and S. Nair, Emerging Insights into Anticancer Chemopreventive Activities of Nutraceutical *Moringa* oleifera: Molecular Mechanisms, Signal Transduction and In Vivo Efficacy, *Curr. Pharmacol. Rep.*, 2020, **6**(2), 38–51, DOI: 10.1007/s40495-020-00210-z.

133 S. Cirmi, N. Ferlazzo, A. Gugliandolo, L. Musumeci, E. Mazzon, A. Bramanti and M. Navarra, Moringin from Moringa Oleifera Seeds Inhibits Growth, Arrests Cell-Cycle, and Induces Apoptosis of SH-SY5Y Human Neuroblastoma Cells through the Modulation of NF-κB and Apoptotic Related Factors, *Int. J. Mol. Sci.*, 2019, **20**(8), 1930, DOI: 10.3390/ijms20081930.